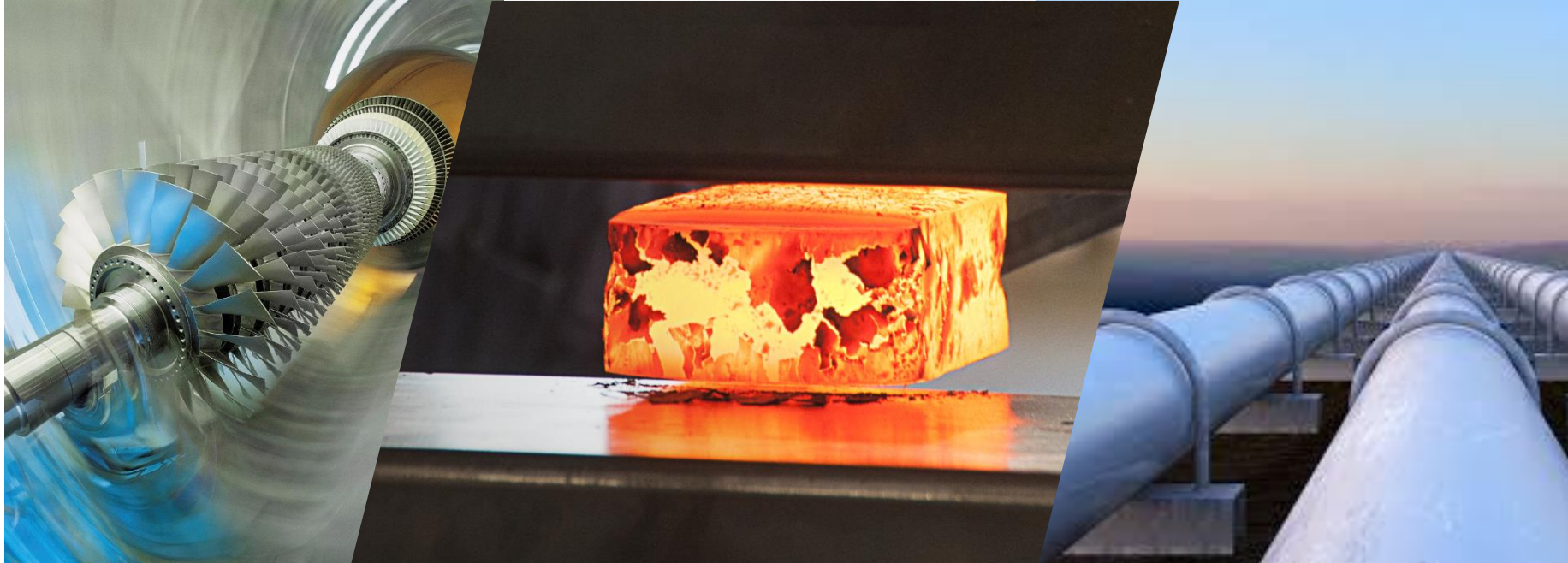


ExtremeMat: Progress update



L.Capolungo

eXtremeMAT Team

- NETL: Michael Gao, Youhai Wen, Madison Wenzlick, Martin Detrois, Tianle Cheng, Fei Xue, Paul Jablonski, Kelly Rose, Marisa Arnold-Stuart, David Alman
- LANL: R. Lebensohn, A. Kumar, A. Chakraborty, L. Capolungo, A. Ruybalid
- ORNL: Y. Yamamoto, Q.Q. Ren, E. Lara-Curzio
- PNNL; R. Devanathan, K.S. Kappagantula
- INL: B. Spencer, L. Munday, M. Glazoff

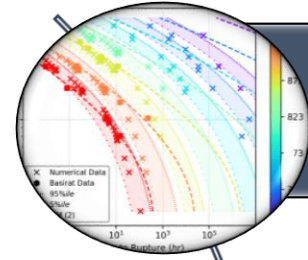
extremeMat: Objectives

General scope: XMAT aims to develop, verify and validate research tools that help the US industry in (i) assessing the failure of steel components subjected to complex non-monotonic loading, (ii) adopting emerging/new steels.

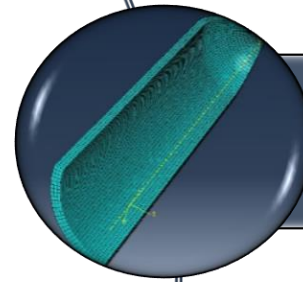
Applications to: conventional austenitic (**347H**, 316H) and ferritic steels (**P91**), XMAT X351..

Conditions: Temperatures from ~500 to 750C, Maximum stresses 100MPa, oxidation in air

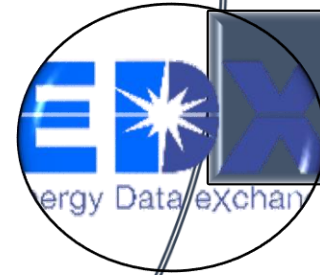
Impact: Reduce the time and cost for alloy qualification and certification.



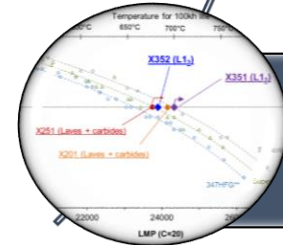
Material lifetime assessment models



Integrated constitutive models



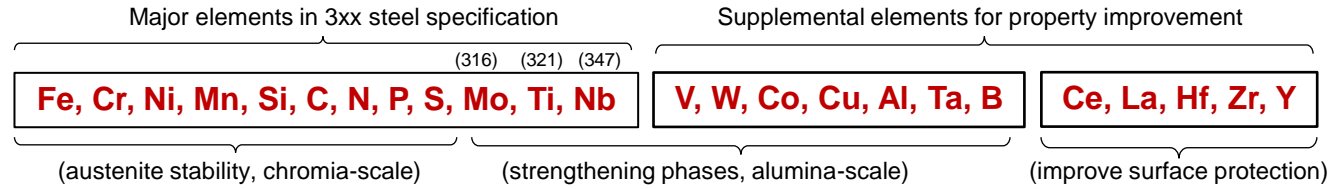
Materials database and analysis tools



Guidelines for the discovery of new alumina forming alloys

Constitutive models are necessary to link microstructure to materials performance

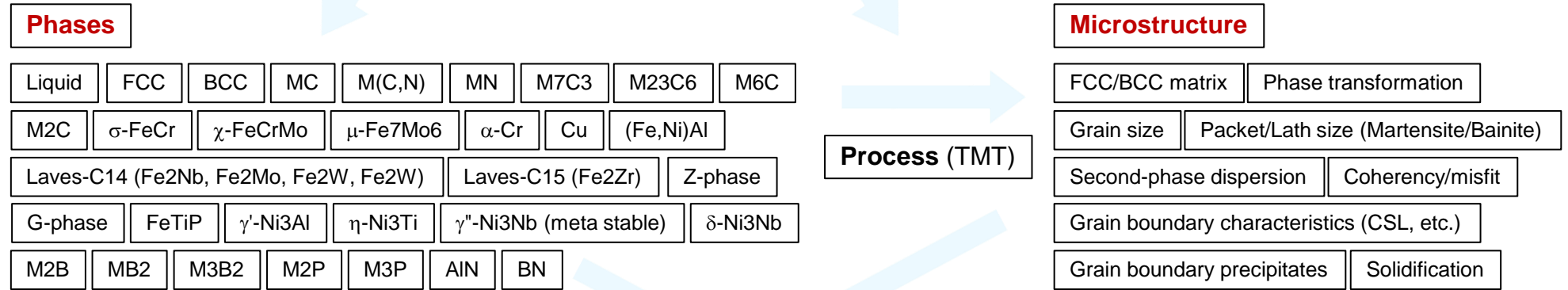
Elements →



Thermodynamics (phase equilibrium)

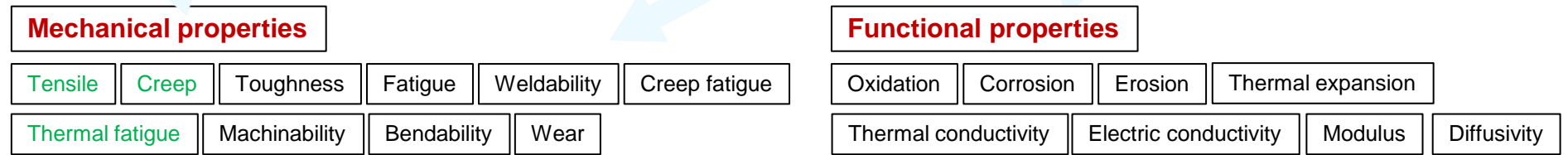
Kinetics (microstructure evolution/stability)

Components →



Prediction (modeling, machine learning, etc.), Validation (experimental, simulation, etc.)

Properties →



Courtesy of Y. Yamamoto ORNL

Mechanistic models can be used to relate composition, microstructure and creep response

Classical Norton-Bailey model, $\dot{\epsilon}^{SS} = A \exp\left(-\frac{Q}{kT}\right) \sigma^n$

Modified BMD model: $\dot{\epsilon}^{SS} = \frac{DEb}{kT} \left(\frac{\sigma - \sigma^{th}}{E}\right)^n \left(\frac{b}{d}\right)^p$

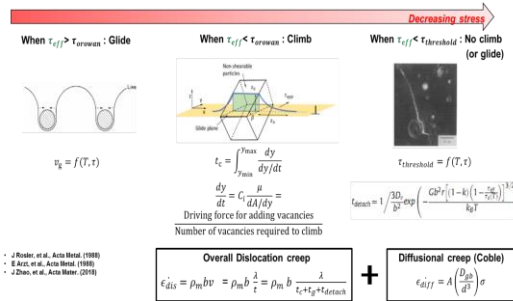
G. Potirniche et al., NEUP project 09-835, final report (2009)

Creep model accounts solutes and precipitates

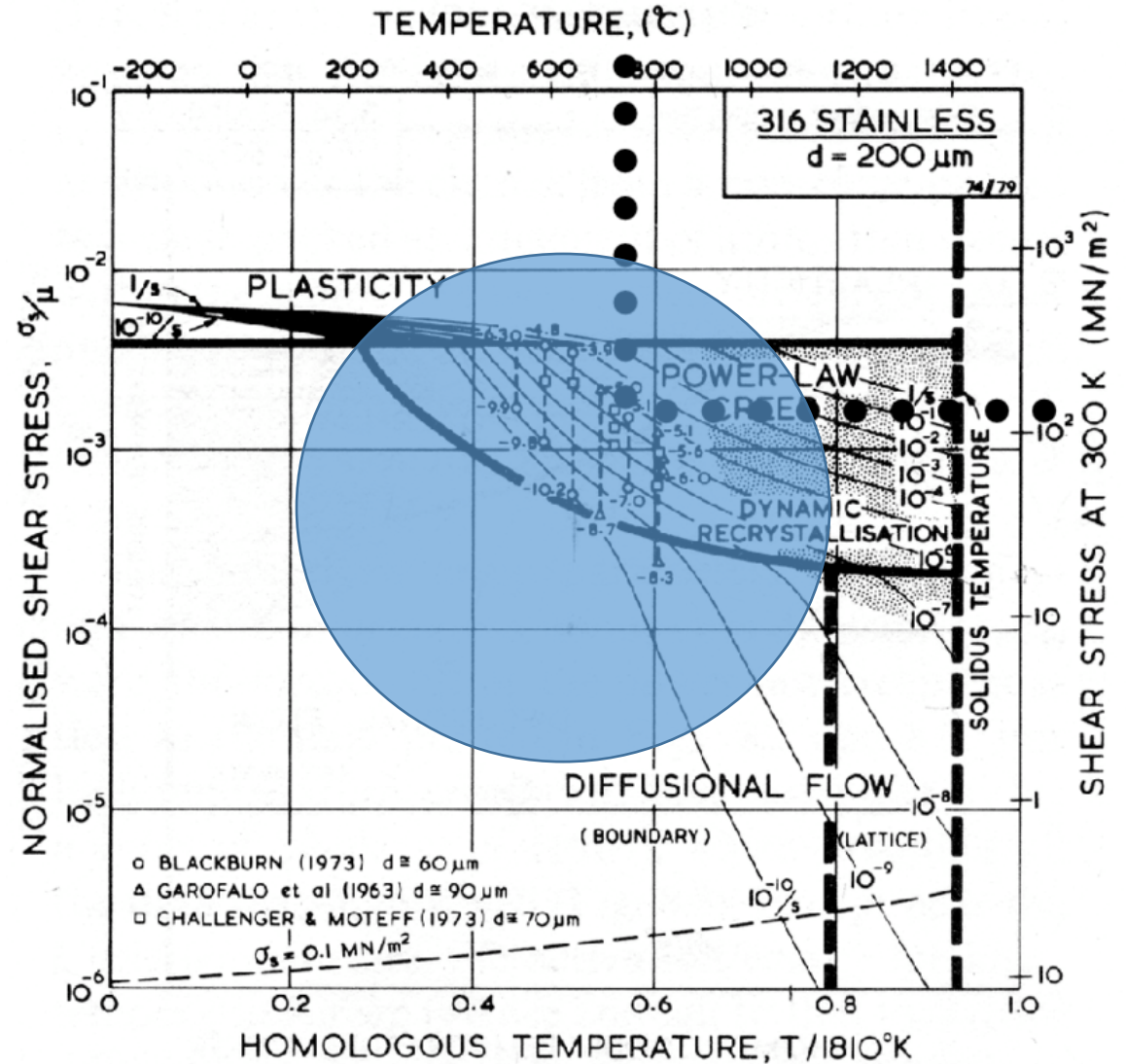
$$\dot{\epsilon}^{SS} = \frac{\pi\Omega kT}{(\alpha GM)^2} \sigma^3 (A(\sigma - \sigma_P)^2 + B(\sigma - \sigma_P) + C) \times \left[\frac{D_{sol} D_L}{2\pi c_0 \ln\left(\frac{r_2}{r_1}\right) D_L + (bkT)^2 \ln\left(\frac{c^*}{c_0}\right) D_{sol}} \right]$$

Fernandez et al., *Advanced Engg Mater*, 22 (2020) 1901355

Microstructure sensitive creep model



Gong and Saboo, DoE project DE-SC0015922, final report (2020)



Mechanistic models can be used to relate composition, microstructure and creep response

Classical Norton-Bailey model, $\dot{\epsilon}^{SS} = A \exp\left(-\frac{Q}{kT}\right) \sigma^n$

Modified BMD model: $\dot{\epsilon}^{SS} = \frac{DEb}{kT} \left(\frac{\sigma - \sigma^{th}}{E}\right)^n \left(\frac{b}{d}\right)^p$

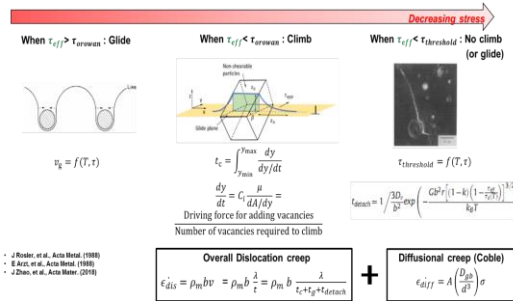
G. Potirniche et al., NEUP project 09-835, final report (2009)

Creep model accounts solutes and precipitates

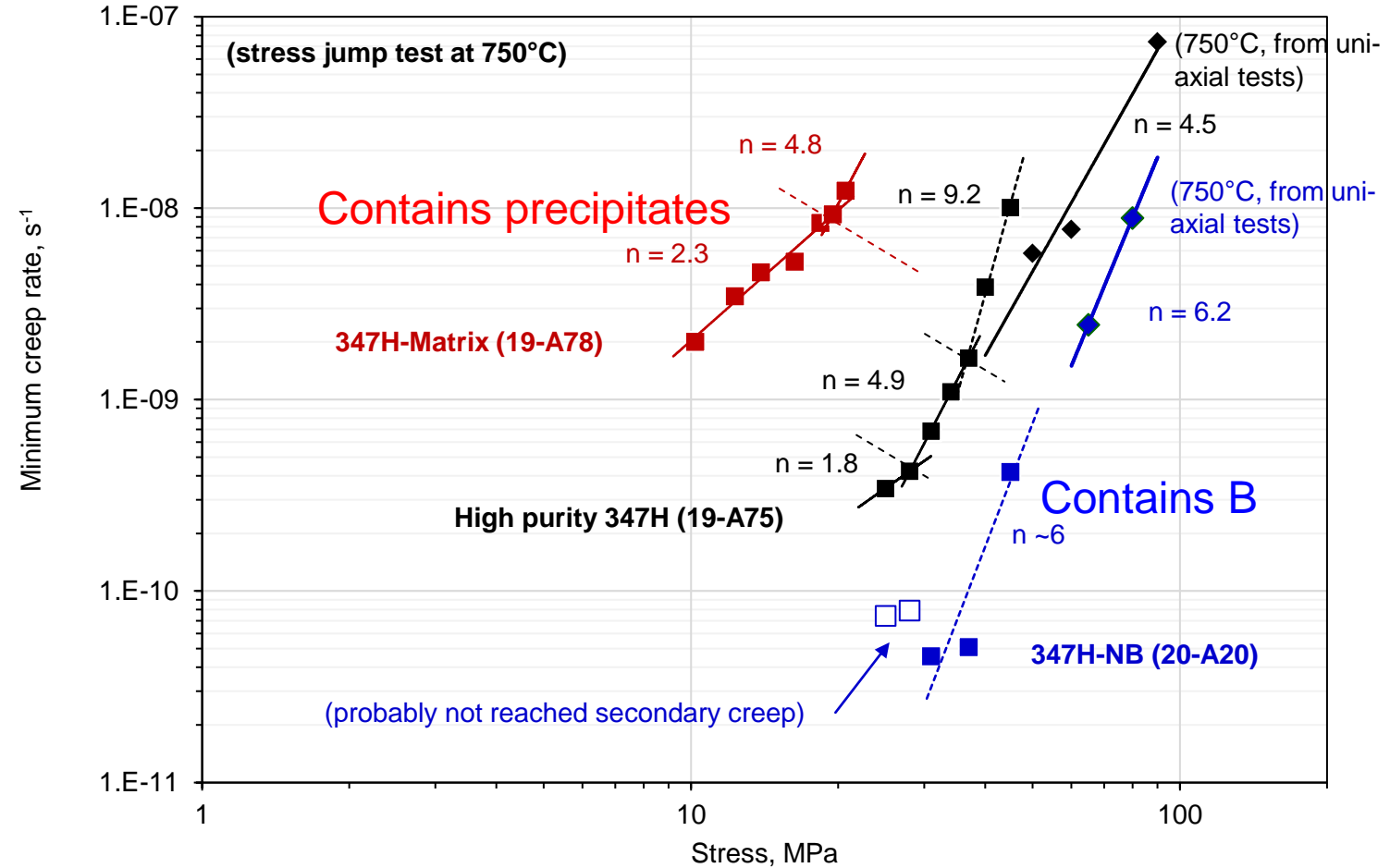
$$\dot{\epsilon}^{SS} = \frac{\pi\Omega kT}{(\alpha GM)^2} \sigma^3 \left(A(\sigma - \sigma_P)^2 + B(\sigma - \sigma_P) + C \right) \times \left[\frac{D_{sol} D_L}{2\pi c_0 \ln\left(\frac{r_2}{r_1}\right) D_L + (bkT)^2 \ln\left(\frac{c^*}{c_0}\right) D_{sol}} \right]$$

Fernandez et al., *Advanced Engg Mater*, 22 (2020) 1901355

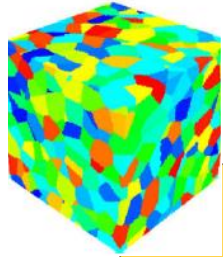
Microstructure sensitive creep model



Gong and Saboo, DoE project DE-SC0015922, final report (2020)

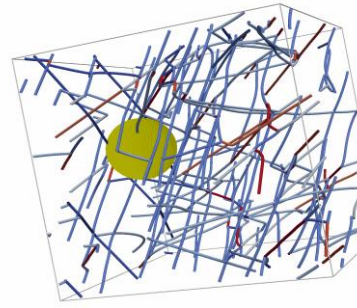


Scientific gaps in relating microstructure composition and performance



Plasticity

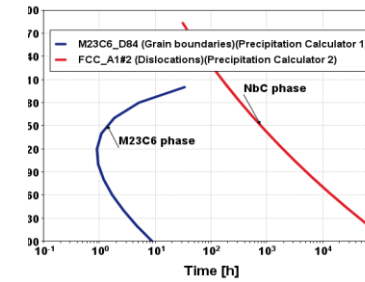
- Dislocation glide
- *Solute vs precipitate strengthening*
- Dislocation climb
- *Vacancy mediated*



Damage

- *Cavity nucleation*
- Cavity growth
- Cavity coalescence

Diagram: Non-Concurrent (Independent) Precipitation of M23C6 (Metastable) and NbC



Aging

- *Second phase evolution*
- *Effect on plastic response and damage*

Effects of **microstructure** (grain size, texture, precipitates, dislocation content, solutes), **stress** (3D, time evolution), **temperature** (time evolution) on material performance

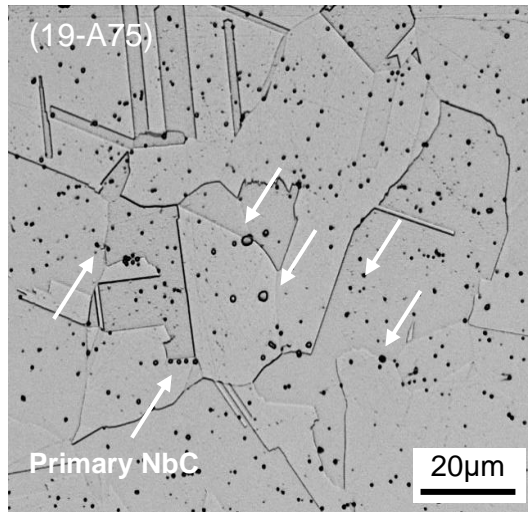
Separating the effects of precipitates and solutes on the creep response and microstructure evolution of 347H

Processing, aging and testing different grades of 347H steels to separate solute vs strengthening and trace elements effects



A 347H plate delivered

| Heat ID | Alloy name | Analyzed chemistry, wt.% (B and N: wppm) | | | | | | | | Remarks |
|-------------------|------------|--|-------|------|------|-------|------|-----|-----|---|
| | | C | Cr | Mn | Nb | Ni | Si | B | N | |
| 19-A75 | 347H | 0.0508 | 18.52 | 0.98 | 0.39 | 11.03 | 0.5 | <5 | 22 | High purity, creep tested at ORNL |
| 19-A92 | 347H | 0.0561 | 18.23 | 0.91 | 0.52 | 10.92 | 0.44 | <5 | 56 | High purity, for tube creep tests |
| 20-A2 | 347H | 0.0541 | 18.72 | 0.98 | 0.3 | 10.84 | 0.44 | <10 | 8 | High purity, tensile and creep at NETL |
| 20-A18 | 347H | 0.0545 | 18.36 | 0.93 | 0.54 | 11.02 | 0.45 | <5 | 11 | Additional high purity 347H |
| 19-A93 | 347H-N | 0.056 | 18.38 | 0.91 | 0.53 | 11.06 | 0.4 | <5 | 184 | N added, for tube creep tests |
| 20-A19 | 347H-N | 0.0531 | 18.37 | 0.93 | 0.51 | 10.97 | 0.42 | <5 | 163 | N added, tensile and creep tests |
| 20-A20 | 347H-N+B | 0.0553 | 18.38 | 0.92 | 0.57 | 10.97 | 0.46 | 11 | 168 | B + N added, tensile and creep tests |
| NIMS-CDS (28B) | Max. | 0.07 | 18.05 | 1.82 | 0.82 | 12.55 | 0.88 | 27 | 284 | Available at https://smds.nims.go.jp/creep/en/ |
| | Min. | 0.05 | 17.26 | 1.66 | 0.49 | 12 | 0.72 | 3 | 160 | |



As-received microstructure (OM)

3 similar alloys with varying N and B content are tested under creep and tensile loads, stress jump tests.

The material systems will be tested in an as received and after aging (750C 336h).

Tests are replicated in different laboratories to ensure consistency of the data.

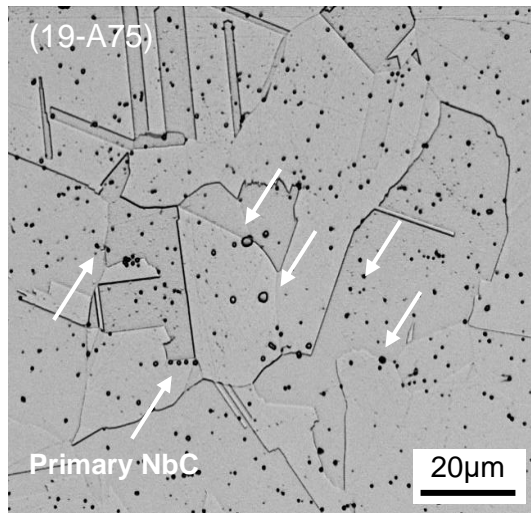
Materials microstructure will be aged to assess thermodynamics and kinetic databases

Processing, aging and testing different grades of 347H steels to separate solute vs strengthening and trace elements effects



A 347H plate delivered

| Heat ID | Alloy name | Analyzed chemistry, wt.% (B and N: wppm) | | | | | | | | Remarks |
|-------------------|------------|--|-------|------|------|-------|------|-----|-----|---|
| | | C | Cr | Mn | Nb | Ni | Si | B | N | |
| 19-A75 | 347H | 0.0508 | 18.52 | 0.98 | 0.39 | 11.03 | 0.5 | <5 | 22 | High purity, creep tested at ORNL |
| 19-A92 | 347H | 0.0561 | 18.23 | 0.91 | 0.52 | 10.92 | 0.44 | <5 | 56 | High purity, for tube creep tests |
| 20-A2 | 347H | 0.0541 | 18.72 | 0.98 | 0.3 | 10.84 | 0.44 | <10 | 8 | High purity, tensile and creep at NETL |
| 20-A18 | 347H | 0.0545 | 18.36 | 0.93 | 0.54 | 11.02 | 0.45 | <5 | 11 | Additional high purity 347H |
| 19-A93 | 347H-N | 0.056 | 18.38 | 0.91 | 0.53 | 11.06 | 0.4 | <5 | 184 | N added, for tube creep tests |
| 20-A19 | 347H-N | 0.0531 | 18.37 | 0.93 | 0.51 | 10.97 | 0.42 | <5 | 163 | N added, tensile and creep tests |
| 20-A20 | 347H-N+B | 0.0553 | 18.38 | 0.92 | 0.57 | 10.97 | 0.46 | 11 | 168 | B + N added, tensile and creep tests |
| NIMS-CDS (28B) | Max. | 0.07 | 18.05 | 1.82 | 0.82 | 12.55 | 0.88 | 27 | 284 | Available at https://smds.nims.go.jp/creep/en/ |
| | Min. | 0.05 | 17.26 | 1.66 | 0.49 | 12 | 0.72 | 3 | 160 | |



As-received microstructure (OM)

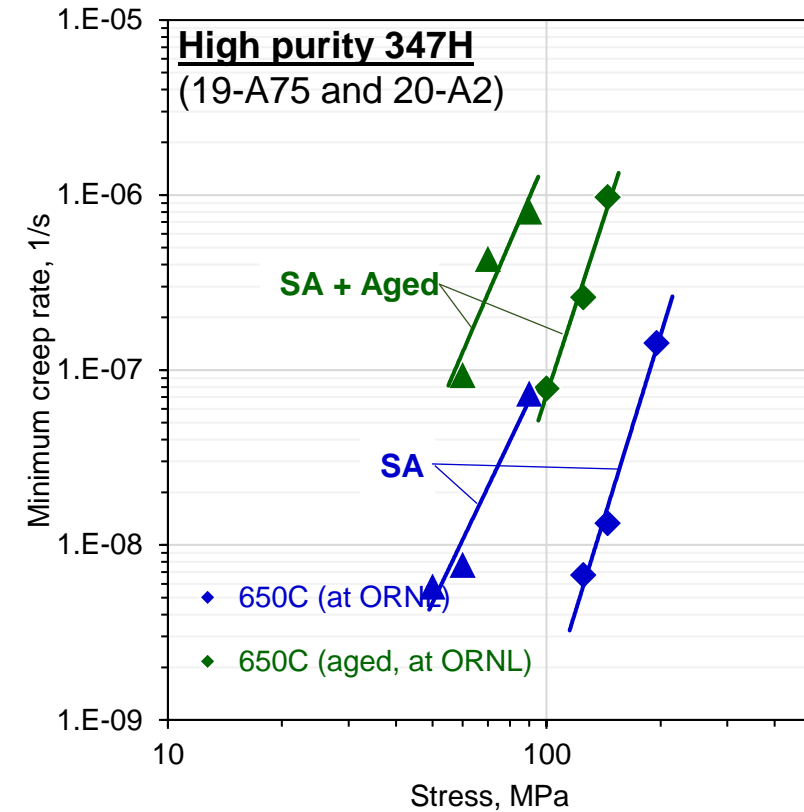
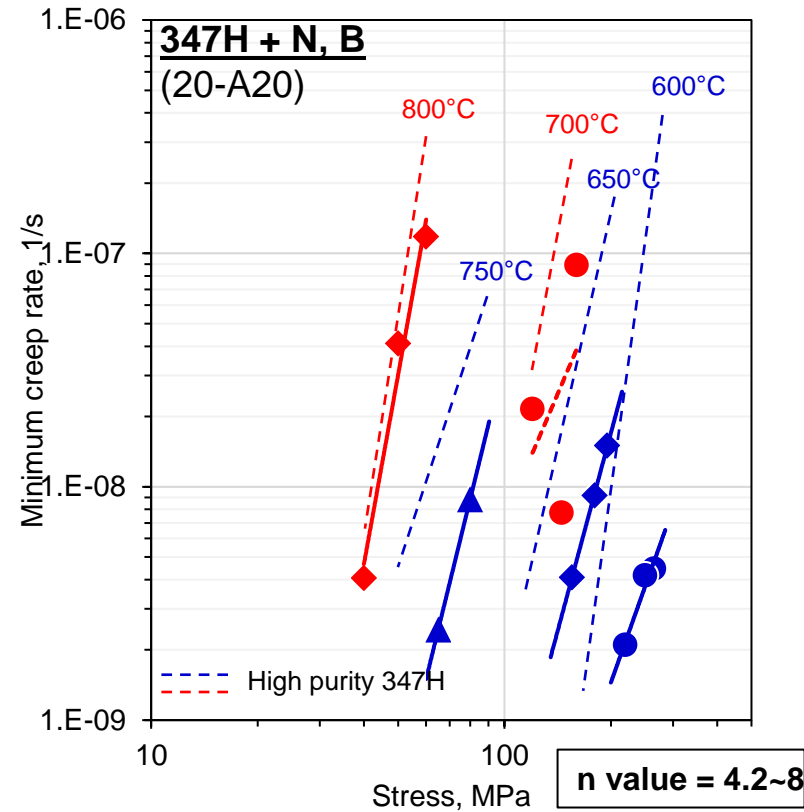
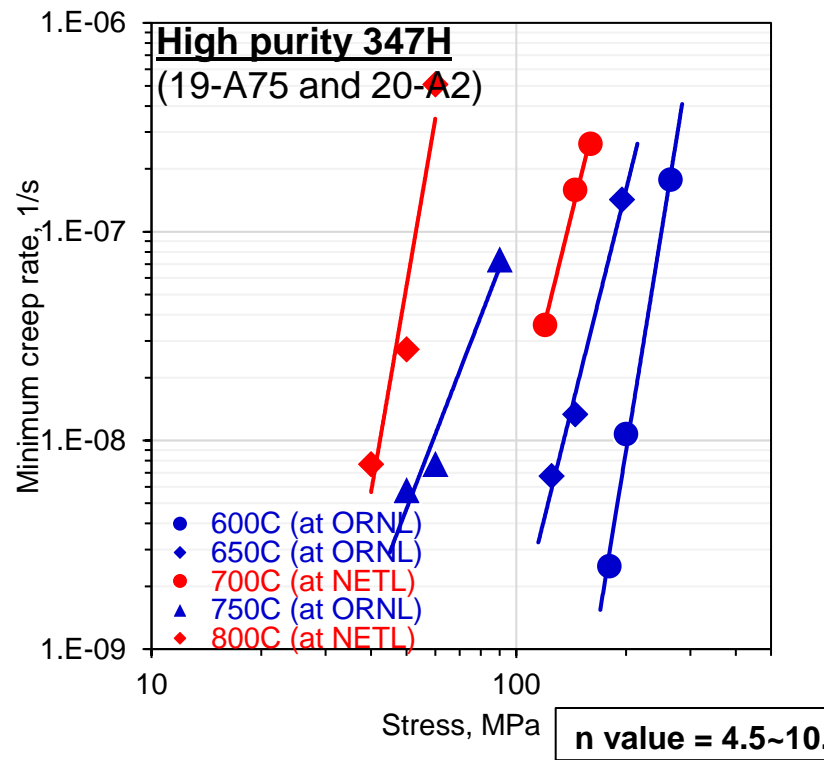
3 similar alloys with varying N and B content are tested under creep and tensile loads, stress jump tests.

The material systems will be tested in an as received and after aging (750C 336h).

Tests are replicated in different laboratories to ensure consistency of the data.

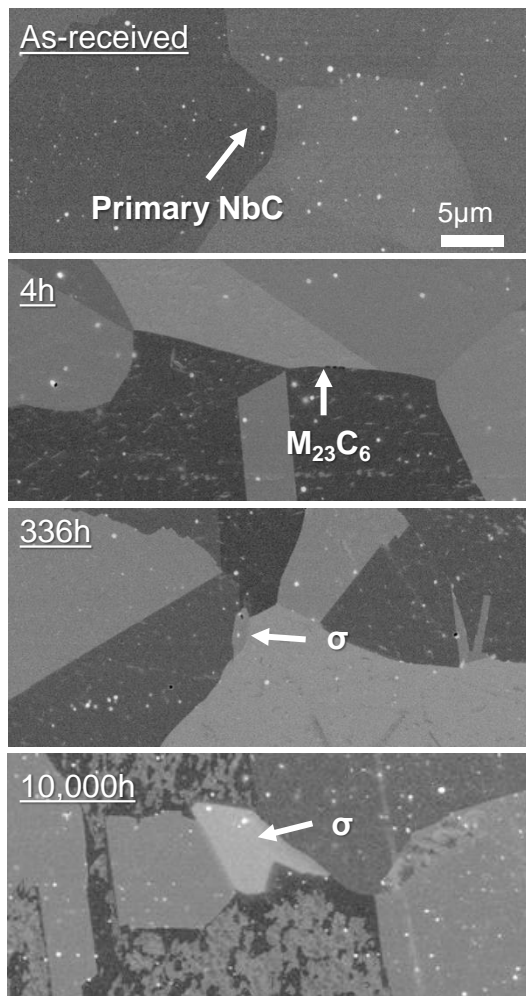
Materials microstructure will be aged to assess thermodynamics and kinetic databases

Aging increases the creep rates, N+B reduce the creep rate



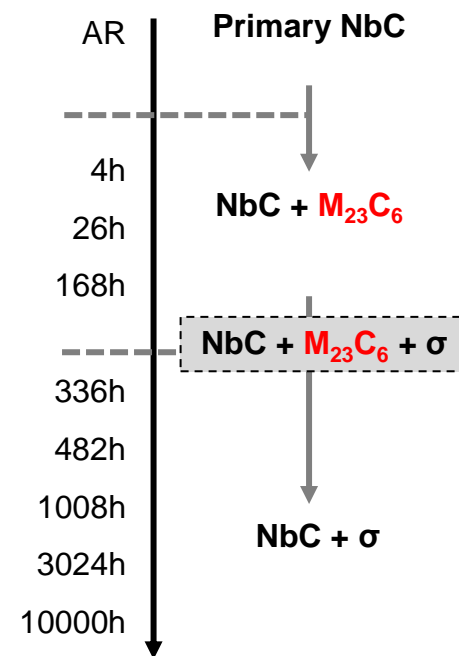
The addition of N +B consistently reduces the creep rate by up to an order of magnitude. Materials aged for 336h at 750C prior to loading exhibit significantly higher creep rates (why? see presentation 1t).

Aging of 347H leads to the formation of secondary NbC, and Sigma phase. N and B stabilize the metastable M₂₃C₆ phase

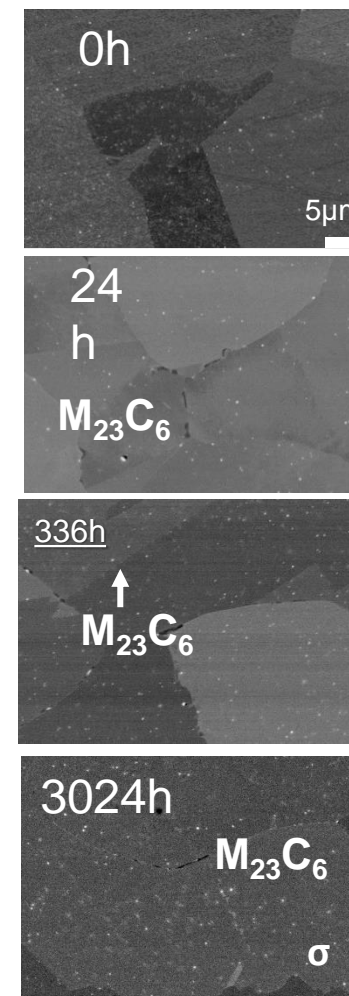


Aged at 750°C (High purity 347H)

Timeline

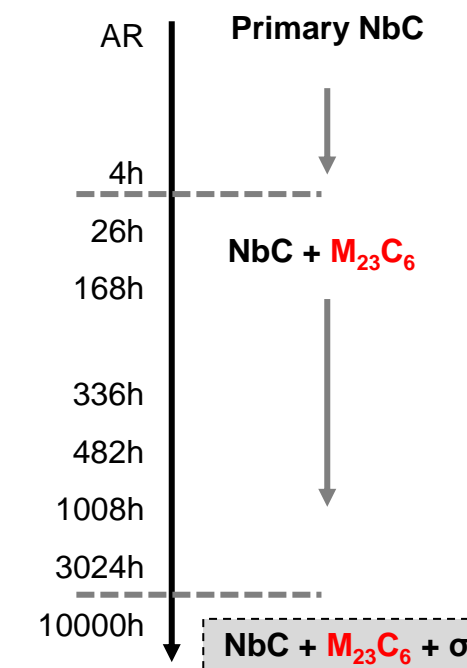


Note; M₂₃C₆ was observed only between 4h and 168h



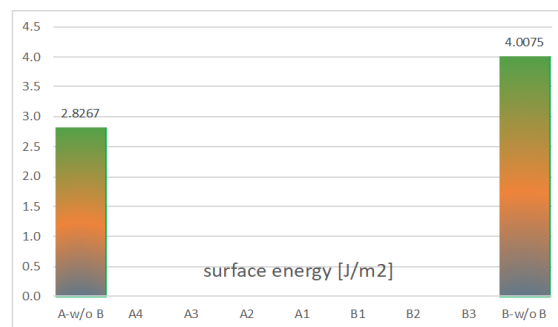
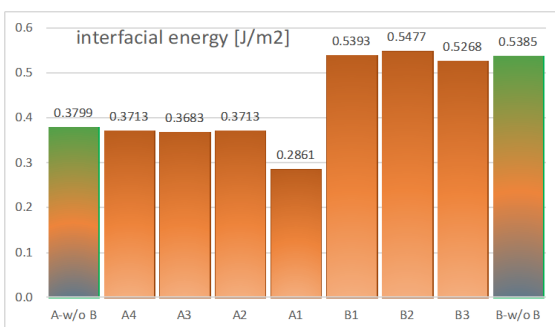
Aged at 750°C (347H_NB, NETL 20-A20)

Timeline



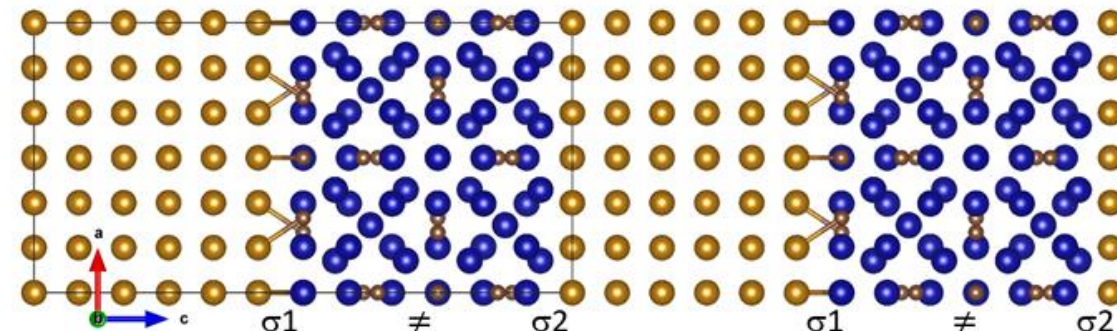
Enhancing thermodynamics databases with DFT simulations to consider elastic energy and trace elements

- **Boron decreases interfacial energy of fcc-Fe/ $M_{23}C_6$ interface by $\sim 0.0938 \text{ J/m}^2$, a very significant value **Boron** prefers to substitute **Carbon** in A-type $Cr_{23}C_6$**
- **B** prefers to **bond with both Fe and Cr, increasing ordering of interface and its stability**. This makes diffusion of C and Cr along/across interface more complicated, **preventing coarsening of $M_{23}C_6$ particles**
- The interfacial energy without B doping for **A-type** is **0.3799 J/m^2** (8 C atoms are at the interface neighboring with both Fe and Cr)
- It is lower than B-type (zero C atoms are at the interface), **0.5385 J/m^2** .
- With B, the **lowest interfacial energy is (A1) 0.2861 J/m^2**



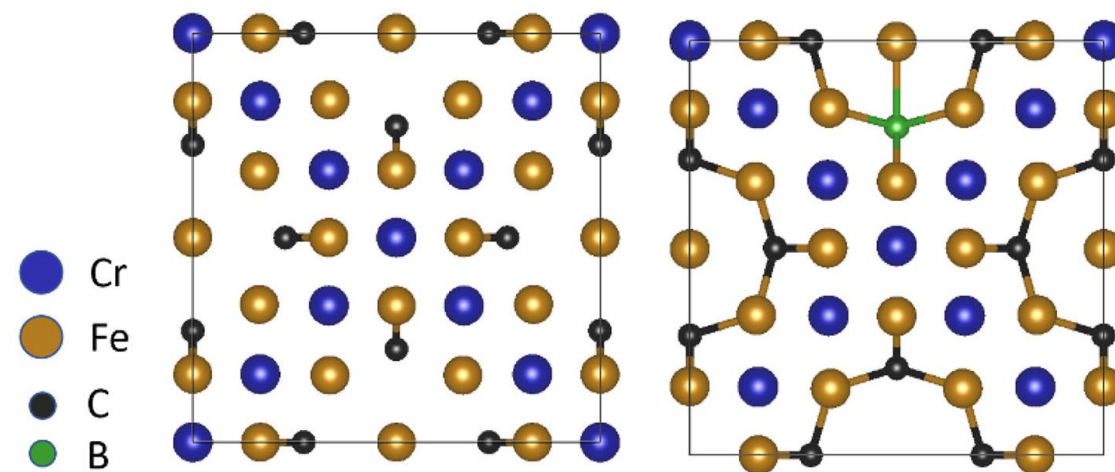
No B

With B



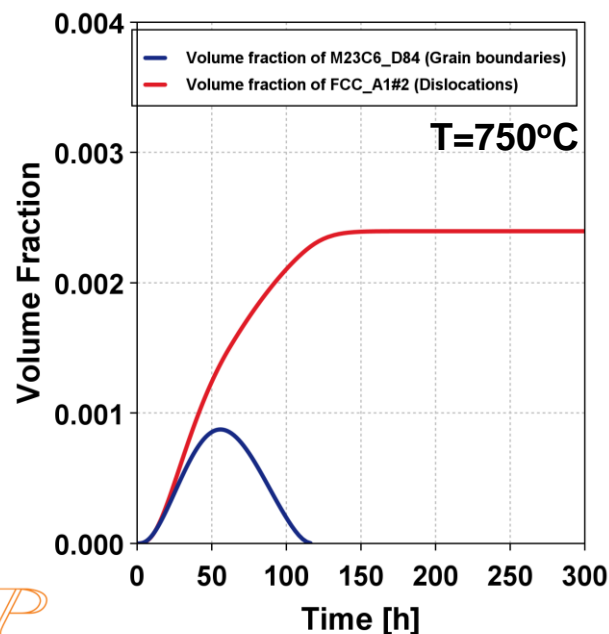
Cr₂₃C₆-fcc Fe interface

With one C replaced with B

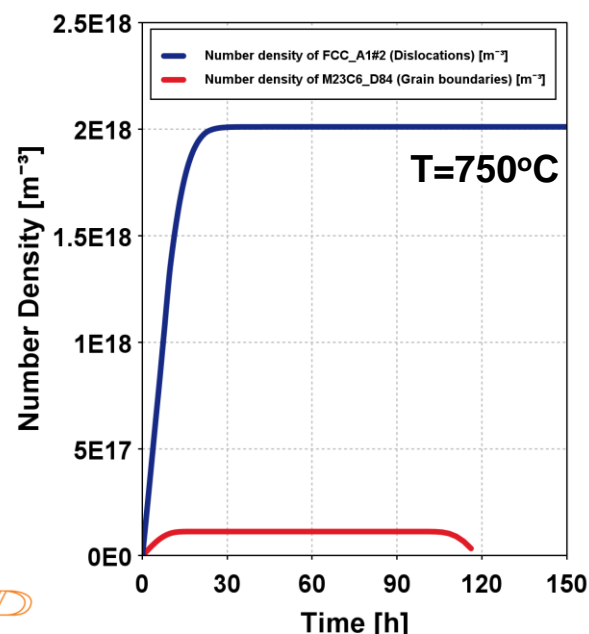


The corrected thermodynamic database allows to predict concurrent precipitation with TC Prisma

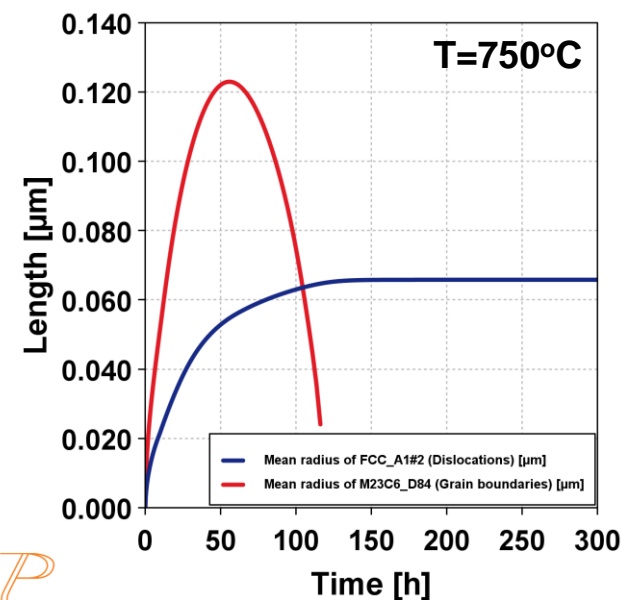
Volume Fractions of M23C6 and NbC



M23C6 & NbC Particle Number Density, m⁻³



M23C6 and NbC Particle Size(s) as Function of Time



Sigma Phase Precipitation - up to 10,000 hours

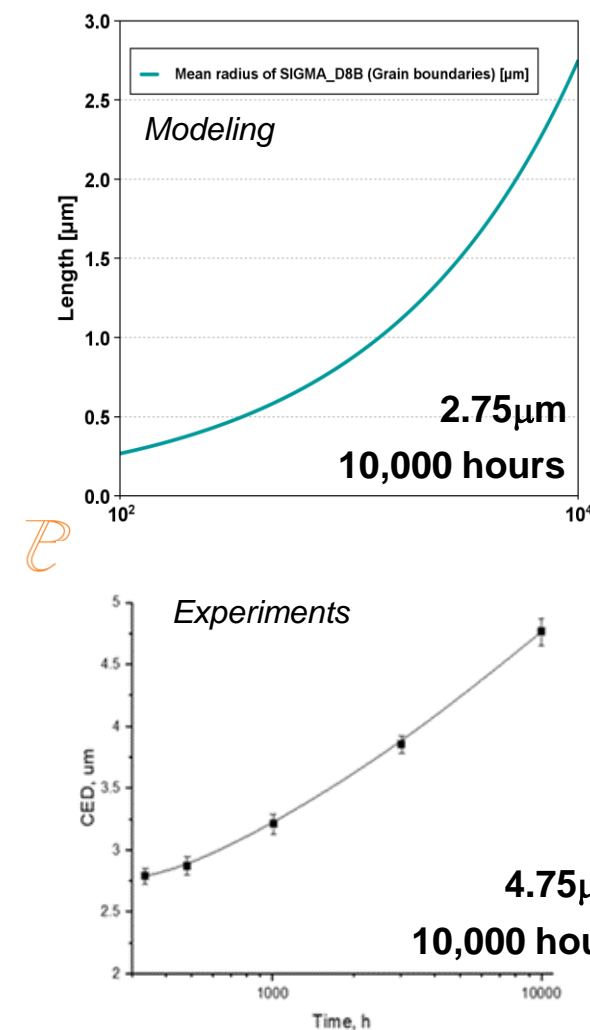


Table Modeling and experimental M₂₃C₆ precipitation data of 347H stainless steels at 750°C

| | Aging time of M ₂₃ C ₆ formation | Volume fraction, % | Number density ^a | Size, μm |
|----------------------------|--|--------------------|-------------------------------------|----------|
| Simulation | 0 through 120 h | 0.09 | $1.1 \times 10^{17} \text{ m}^{-3}$ | 0.125 |
| Experimental ³⁷ | 4 h, 24 h, and 168 h | 0.10 | $4.7 \times 10^{14} \text{ m}^{-3}$ | 0.480 |

^aThe original experimental result, $6.0 \times 10^9 \text{ m}^{-2}$, was presented in $\{\text{m}^{-2}\}$. If recalculated into $\{\text{m}^{-3}\}$, we will obtain the value given in Table III, i.e., $4.7 \times 10^{14} \text{ m}^{-3}$.

The kinetics of concurrent precipitation are captured.

The volume fractions of precipitates are captured.

Number densities and size are off

Quantifying the effects of microstructure on performance variability during creep

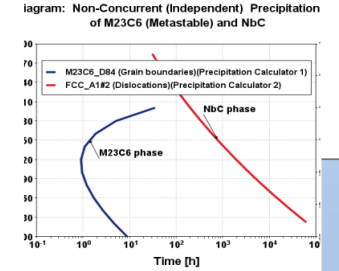
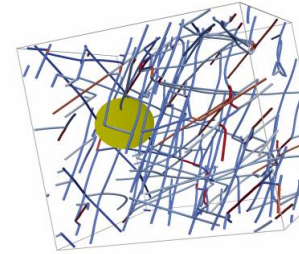
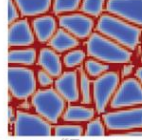
Mechanistic models can be used to relate composition, microstructure and creep response

Classical Norton-Bailey model, $\dot{\epsilon}^{SS} = A \exp\left(-\frac{Q}{kT}\right) \sigma^n$

Modified BMD model: $\dot{\epsilon}^{SS} = \frac{DEb}{kT} \left(\frac{\sigma - \sigma^{th}}{E}\right)^n \left(\frac{b}{d}\right)^p$

G. Potirniche et al., NEUP project 09-835, final report (2009)

See presentation by Aritra Chakraborty



Plasticity

- Dislocation glide
- Solute vs precipitate strengthening
- Dislocation climb
- Vacancy mediated

Damage

- Cavity nucleation
- Cavity growth
- Cavity coalescence

Aging

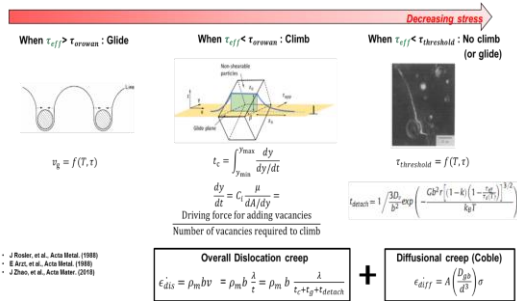
- Second phase evolution
- Effect on plastic response and damage

Creep model accounts solutes and precipitates

$$\dot{\epsilon}^{SS} = \frac{\pi\Omega kT}{(\alpha GM)^2} \sigma^3 (A(\sigma - \sigma_p)^2 + B(\sigma - \sigma_p) + C) \times \left[\frac{D_{sol} D_L}{2\pi c_0 \ln\left(\frac{r_2}{r_1}\right) D_L + (bkT)^2 \ln\left(\frac{c^*}{c_0}\right) D_{sol}} \right]$$

Fernandez et al., Advanced Engg Mater, 22 (2020) 1901355

Microstructure sensitive creep model

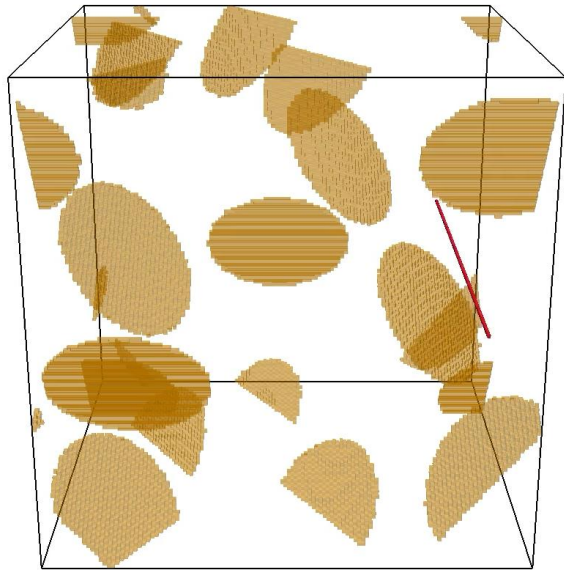


Gong and Saboo, DoE project DE-SC0015922, final report (2020)

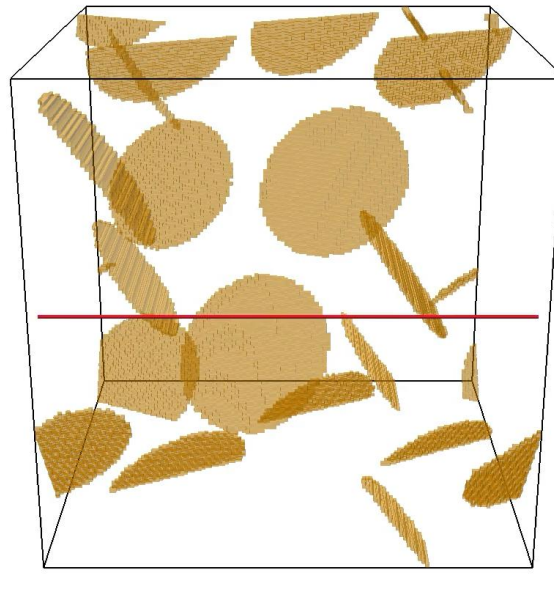
Effects of **microstructure** (grain size, texture, precipitates, dislocation content, solutes), **stress** (3D, time evolution), **temperature** (time evolution) on material performance

Precipitate strengthening

No cross-slip



Cross-slip



Dispersed Barrier Hardening: based on mean spacing between defects.

$$Ds = amb\sqrt{Nd}$$

Friedel-Kroupa-Hirsch: based on elastic interactions between SIA loops and straight dislocations.

$$Ds = a \frac{mb^0 RN^{\frac{3}{2}}}{8}$$

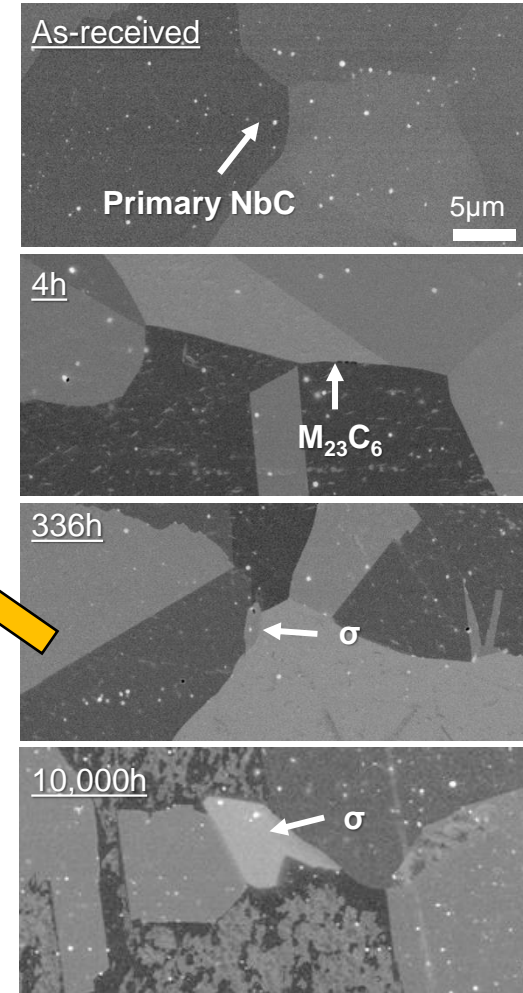
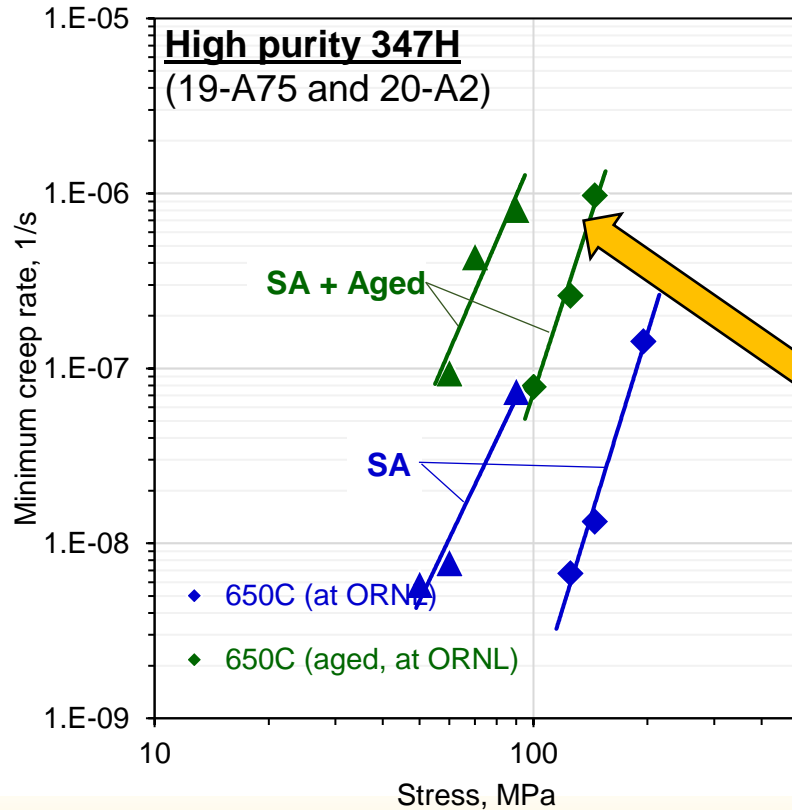
Bacon-Kocks-Scattergood: based on random array of spherical obstacles. Includes elastic self-interaction.

$$Ds = a \frac{mb}{2\rho L} \left[\ln\left(\frac{L}{b}\right) \right]^{1/2} \left[\ln\left(\frac{d'}{b}\right) + 0.7 \right]^{3/2}$$

Precipitates are overwhelmingly seen as strengtheners.

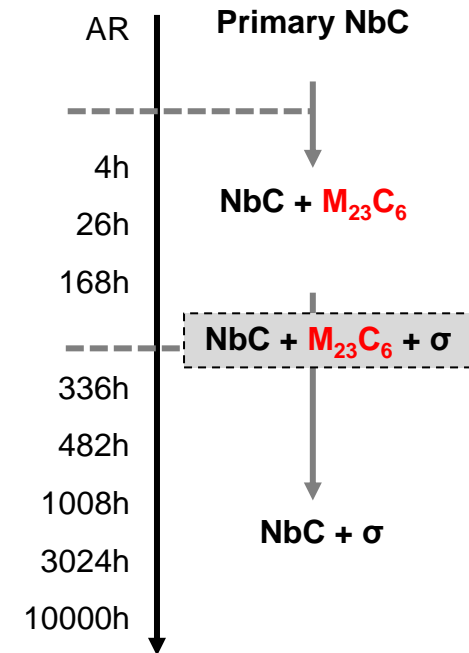
R. Santos-Guemes et al. JMPS 2021

Precipitate “strengthening”



Aged at 750°C
(High purity 347H)

Timeline

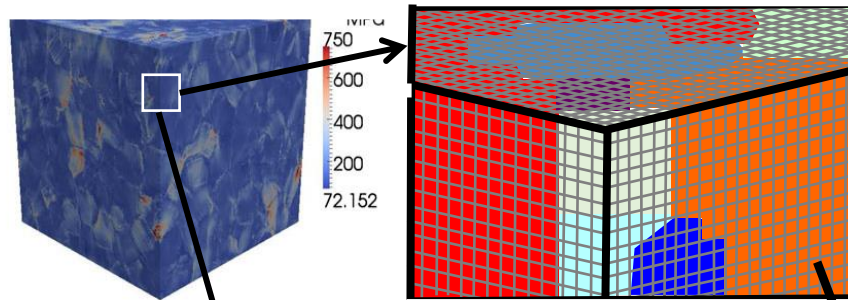


Note; $M_{23}C_6$ was observed only between 4h and 168h

Precipitates are overwhelmingly seen as strengtheners.

Then, how does one rationalize the observed creep response of aged vs non aged systems? Is it due to the loss of solute? How is this compensated by dislocation motion

Elasto-Visco-Plastic fast Fourier Transform (XMAT-EVPFFT) modeling framework



(b) Von mises effective stress

(Lebensohn et al., IJP, 2012)

Strain-rate at a material point: $\dot{\epsilon}(x) = \dot{\epsilon}^e(x) + \dot{\epsilon}^{vp}(x)$

Total plastic strain rate, $\dot{\epsilon}^{vp} = \dot{\epsilon}^g + \dot{\epsilon}^c + \dot{\epsilon}^{Diff}$

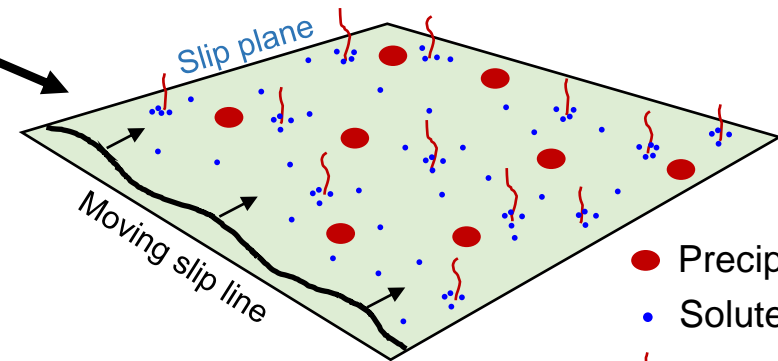
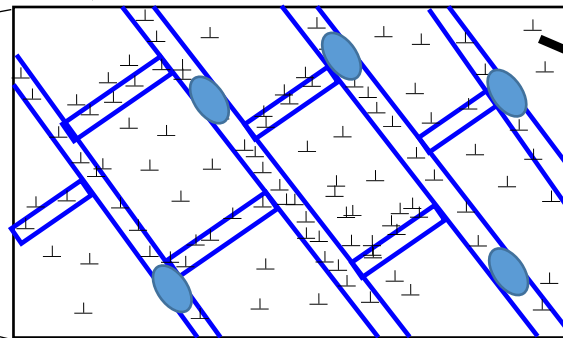
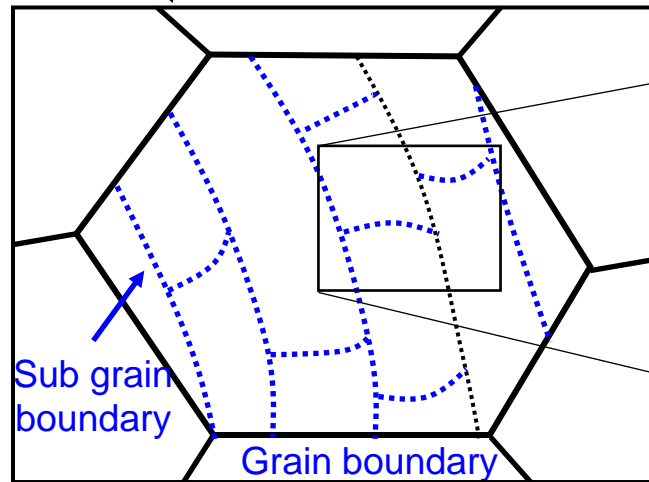
due to glide

$$\dot{\epsilon}^g = \sum_s m^s \bar{\gamma}^s$$

due to climb

$$\dot{\epsilon}^c = \sum_s C^s \bar{\beta}^s$$

due to diffusion



- Precipitates
- Solutes
- ⌋ Dislocation junction

Climb can mediate the bypass of precipitates

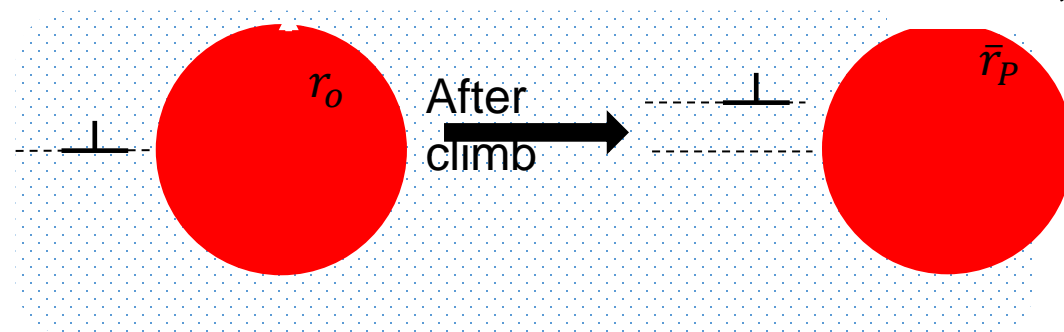
Dislocation glide velocity, $v^s = \frac{\lambda^s}{t_w^s + t_t^s}$

Mean interspacing: $\left(\frac{1}{\lambda^s}\right)^\alpha = \left(\frac{1}{\lambda_\rho^s}\right)^\alpha + \left(\frac{1}{\lambda_{sg}^s}\right)^\alpha + \sum \left(\frac{1}{\lambda_{P_i}^s}\right)^\alpha$

Dislocation mean free path for precipitates:

$\frac{1}{\lambda_P^s} = \alpha_P \sqrt{N_P \bar{d}_P}$ → Effective precipitate size
 → Number density

$$\bar{d}_P = d_0 \left(1 - \frac{t_w^s v_c^s}{d_0} \right)$$



As dislocations wait at precipitates, sufficient time maybe given for them to climb over part of precipitates (aging mechanisms for precipitate)

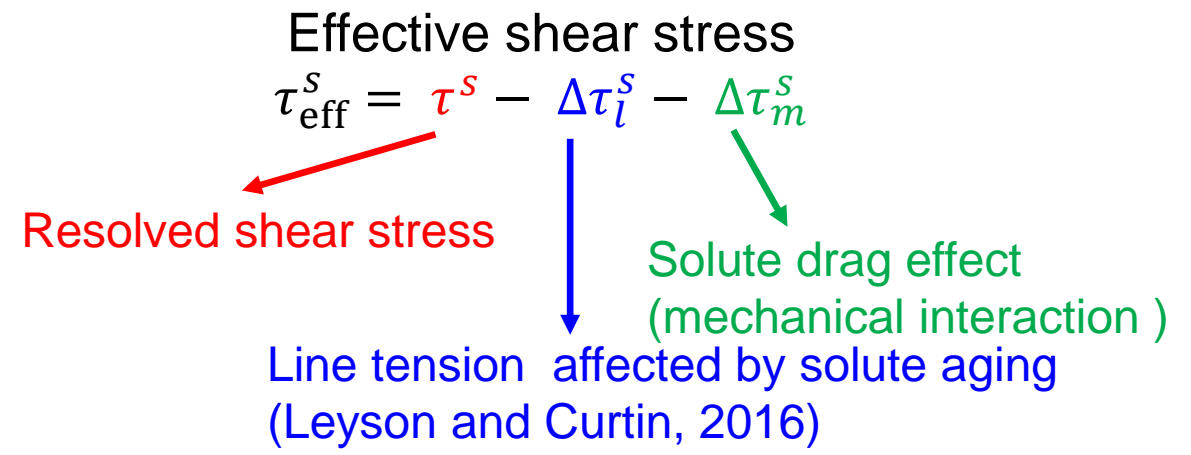
$$v_c^s = \frac{\Omega}{b} \left(z_v^s D_v C_v^{th} \left[\exp \left(\frac{\Omega \bar{\tau}_{climb}^s}{kT} - 1 \right) \right] \right)$$

Solute effects have multiple effects on dislocation glide

$$t_{w,i,g}^s = \frac{1}{v_{a,i}^s} \exp\left(\frac{\Delta G_{0,i}}{kT} \left(1 - \left(\frac{\tau_{eff}}{\tau_c^s}\right)^p\right)^q\right)$$

i : Dislocations or precipitates

Waiting time for thermally activated dislocation glide



Critical resolved shear stress

$$\tau_c^s = \tau_0^s + \left(\tau_{CW}^n + \tau_{L,sub}^n + \tau_{L,int}^n + \sum_i \tau_{Pi}^n \right)^n$$

Lattice friction

Cell-structure strengthening

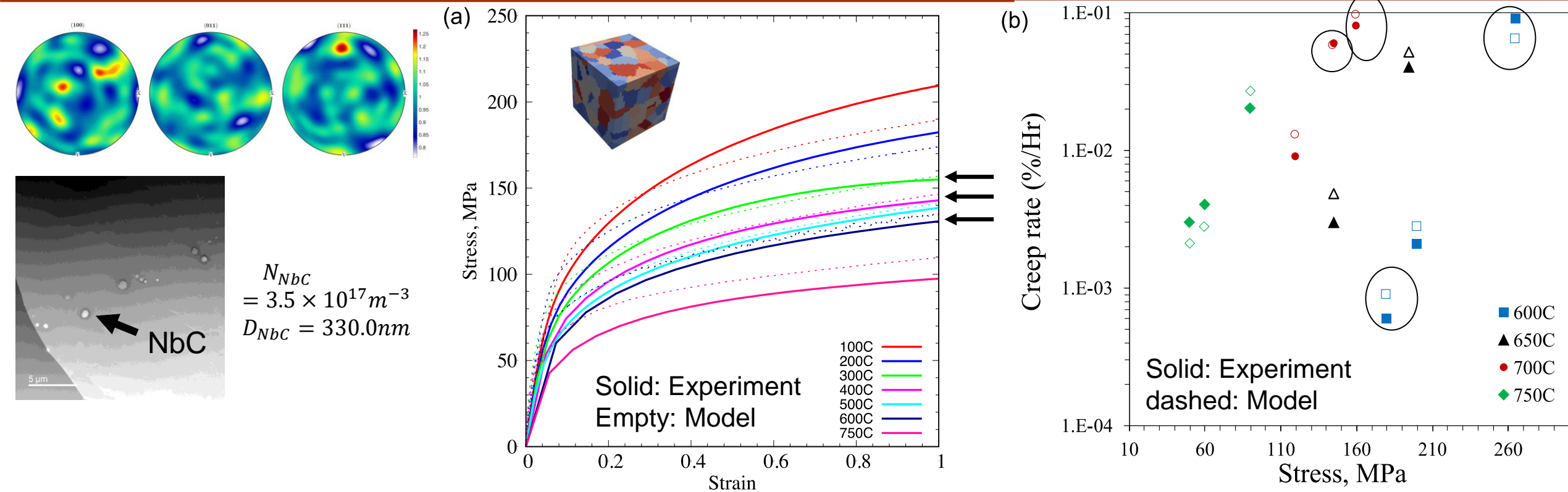
Substitutional solutes induced resistance

Interstitial solutes induced resistance

Precipitate hardening

Strengthening is driven by the interplay between solute strengthening, dynamics strain aging, precipitate strengthening, climb mediated

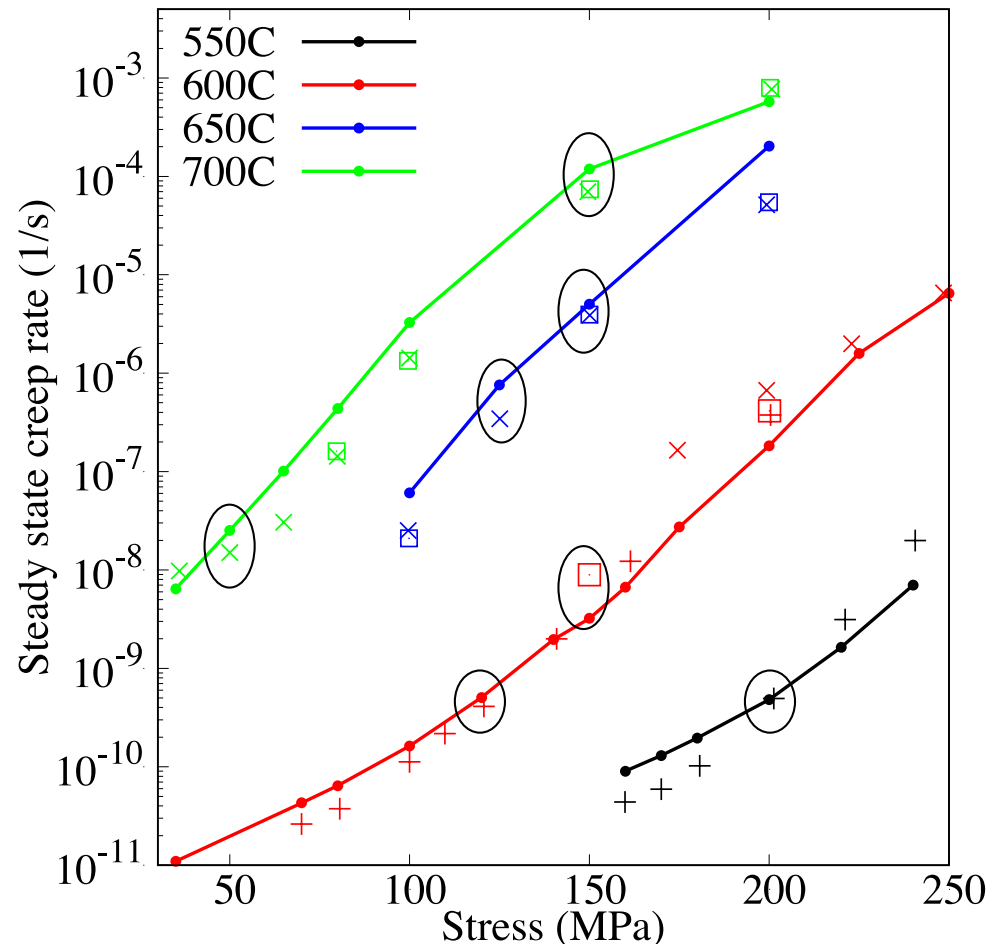
The polycrystalline framework can simultaneously predict creep and tensile loading of 347H



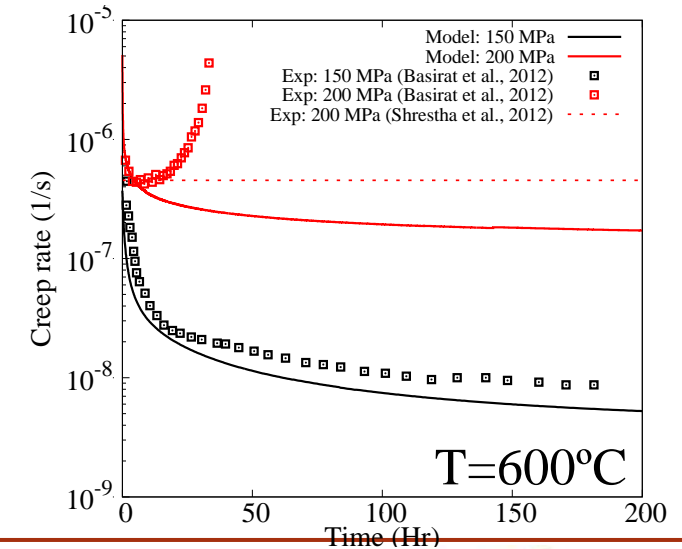
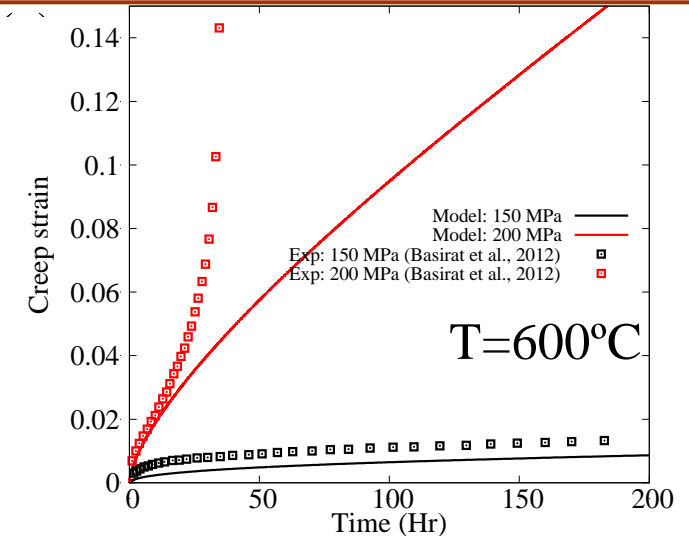
The model captures the experimentally measured stress-strain and creep responses.

The model is tested both as an interpolator or extrapolator.

The same framework can be applied to a ferritic steel (Gr91)



□: Basirat et al. (2012) ×: Shrestha et al. (2012)
+ : Kimura et al. (2009) ●—: Model



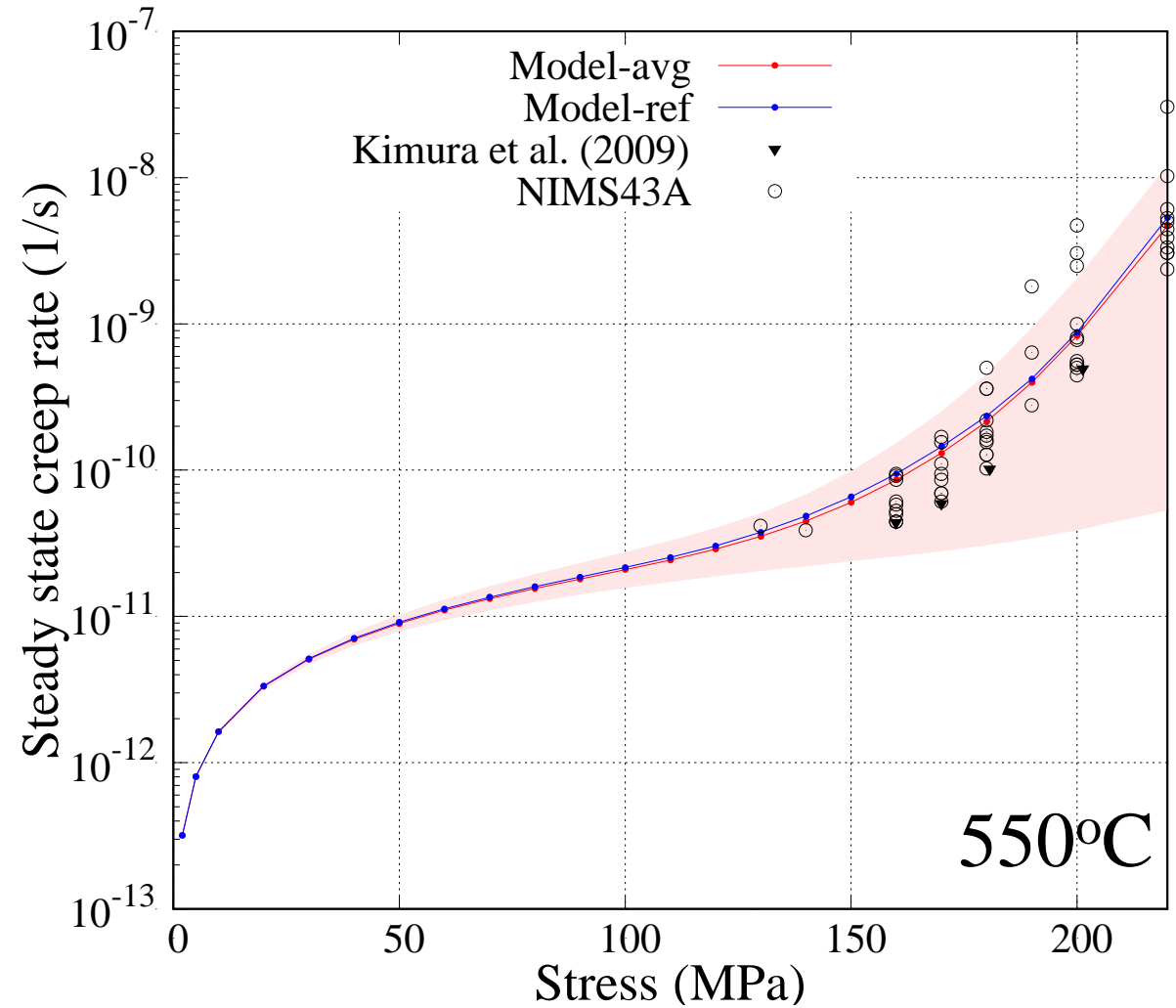
The variability in creep response induced microstructure depends on loading conditions

| Parameter | Values |
|---|-----------------------------|
| Dislocation density within the cells, ρ_{ci} (m^{-2}) | [1,2,4,6,8]. 10^{12} |
| Dislocation density at the cell walls: ρ_{cw} (m^{-2}) | [1,2.5, 5, 10]. ρ_{ci} |
| Precipitate number density, N_p (m^{-3}) | [1,2,3,4,6] |
| Precipitate size, D_p ($10^{-9}m$) | [25,37,50] |

As precipitate content is changed, the solute content in the matrix is updated

While the model was calibrated against limited number of tests, it can rationalize the wide spread in reported secondary creep rates.

Microstructure descriptors affects the response dominantly in the dislocation creep regime



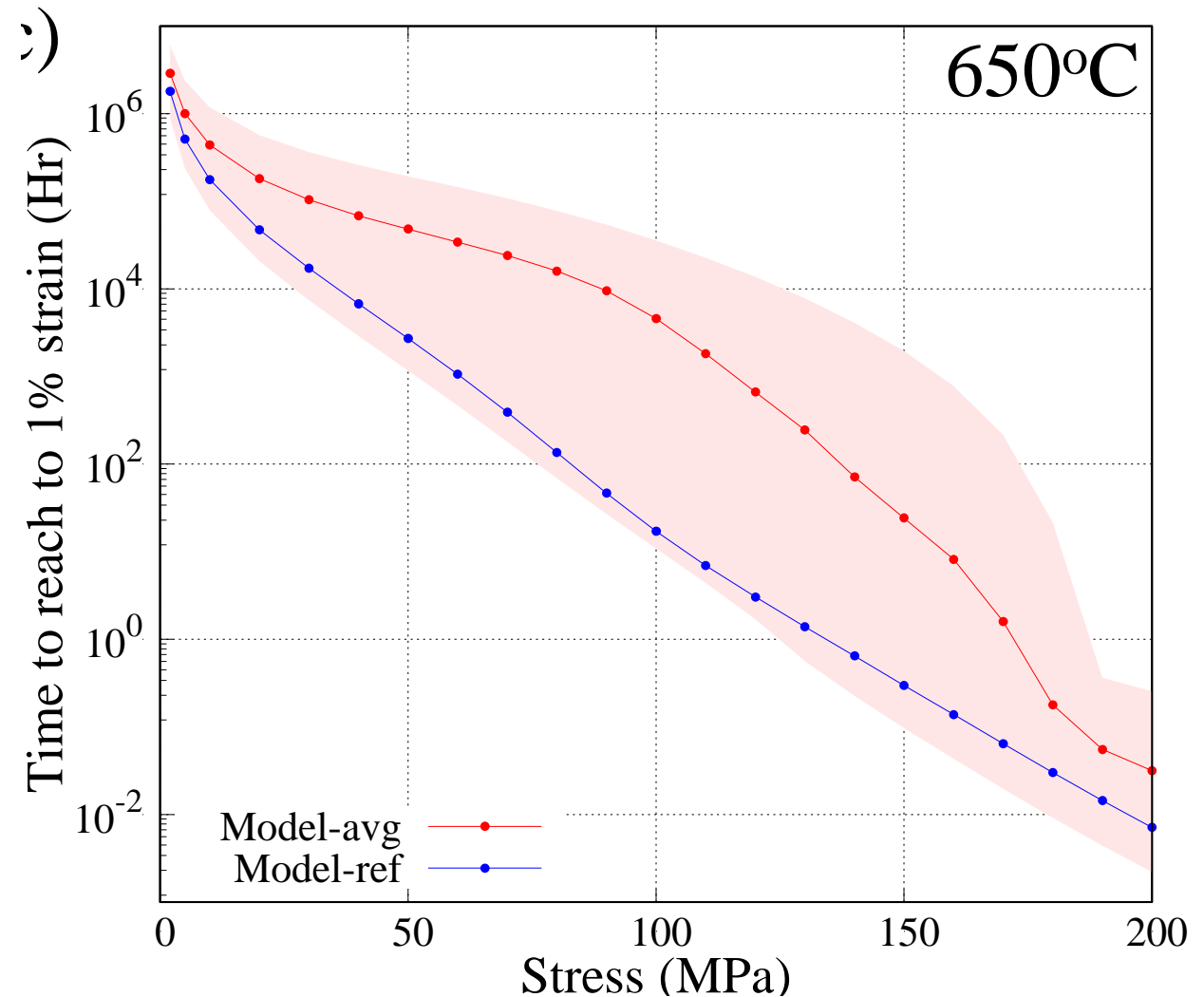
The variability in creep response induced microstructure depends on loading conditions

| Parameter | Values |
|---|-----------------------------|
| Dislocation density within the cells, ρ_{ci} (m^{-2}) | [1,2,4,6,8]. 10^{12} |
| Dislocation density at the cell walls: ρ_{cw} (m^{-2}) | [1,2.5, 5, 10]. ρ_{ci} |
| Precipitate number density, N_p (m^{-3}) | [1,2,3,4,6] |
| Precipitate size, D_p ($10^{-9}m$) | [25,37,50] |

As precipitate content is changed, the solute content in the matrix is updated

While the model was calibrated against limited number of tests, it can rationalize the wide spread in reported secondary creep rates.

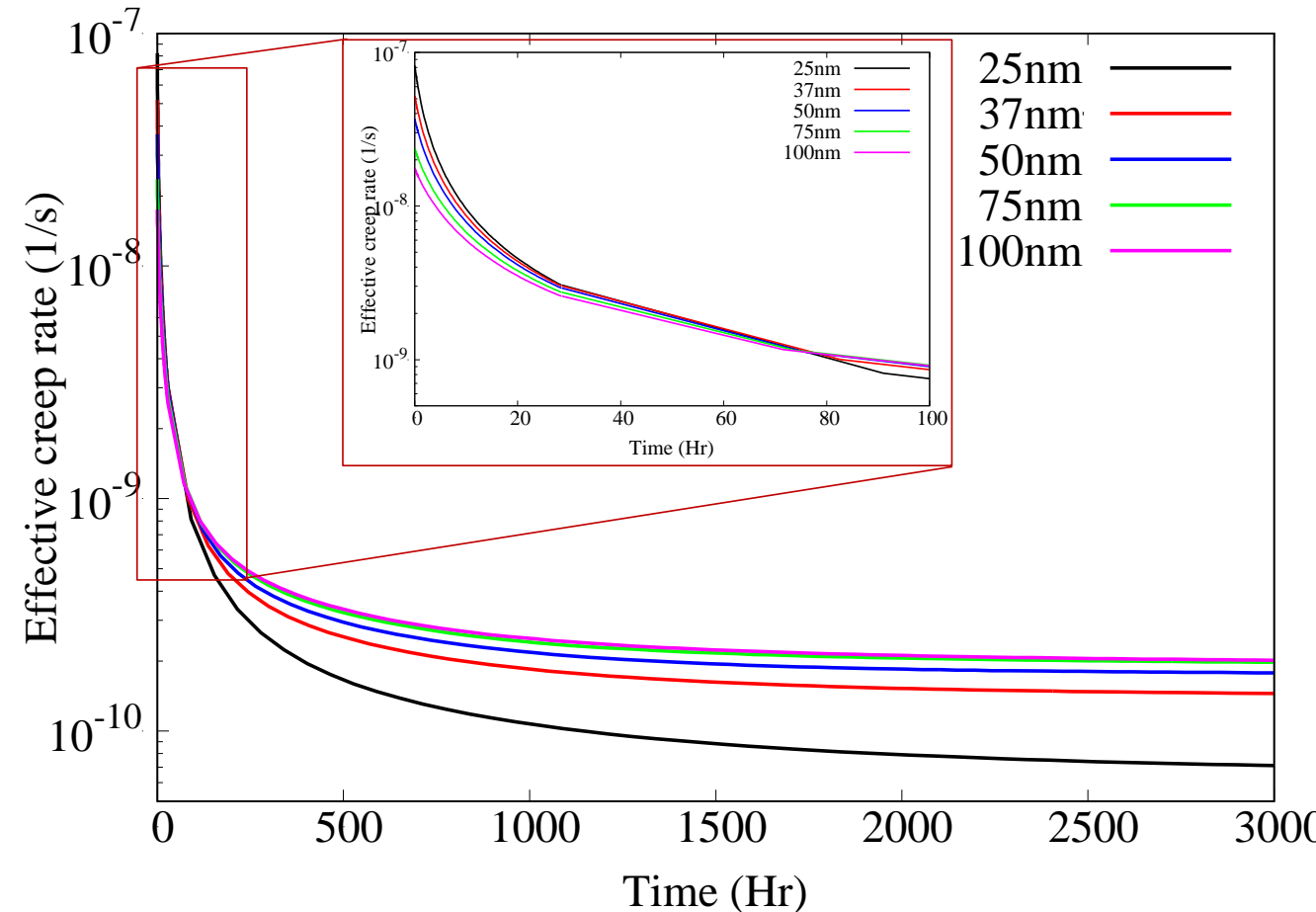
Microstructure descriptors affects the response dominantly in the dislocation creep regime



Precipitate “strengthening”

Gr91 subjected to creep at 600C under
100MPa stress

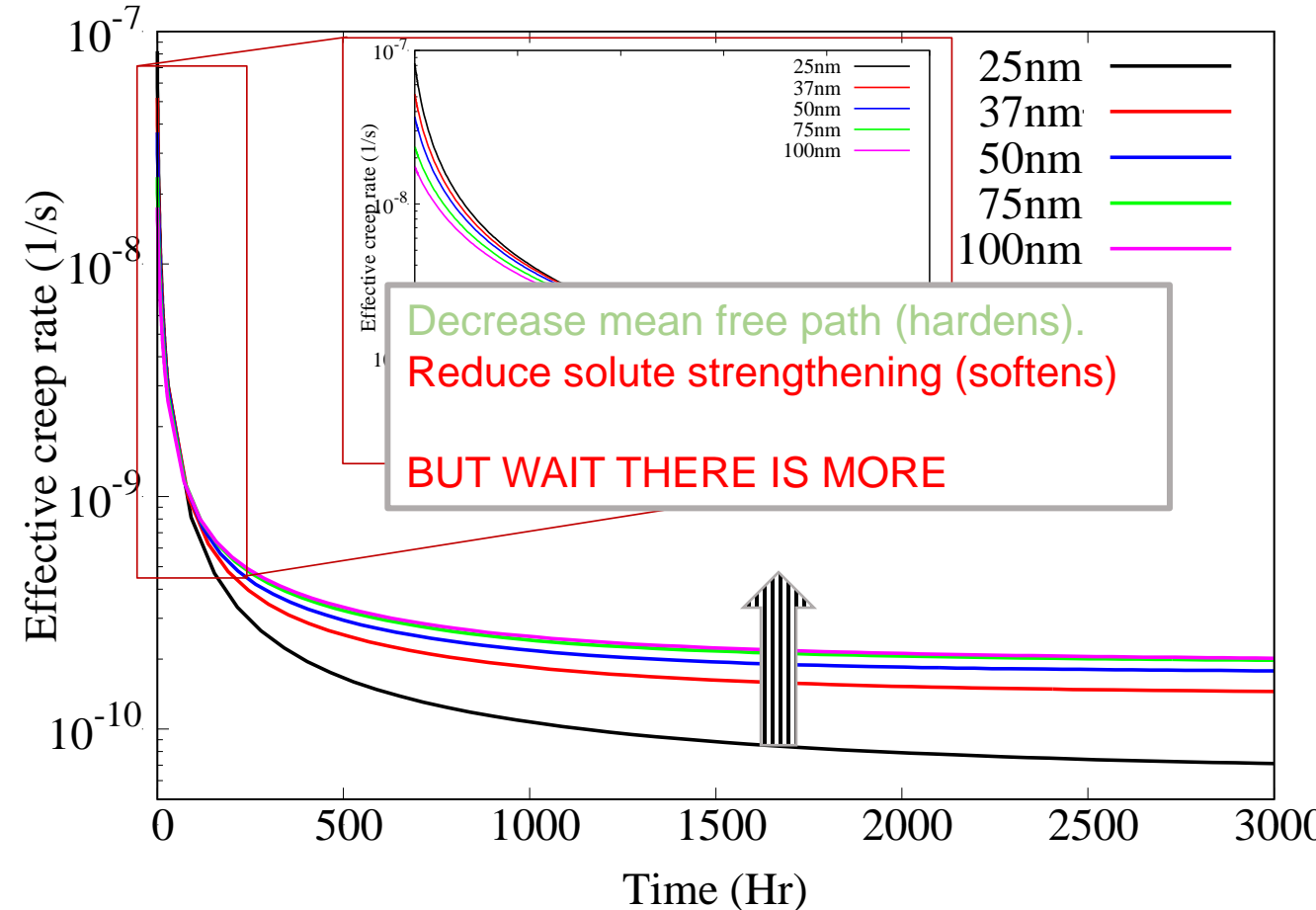
Increasing the size of precipitates which
reduces the solute content in the matrix can
lead to an increase in the creep rate



Precipitate “strengthening”

Gr91 subjected to creep at 600C under 100MPa stress

Increasing the size of precipitates which reduces the solute content in the matrix can lead to an increase in the creep rate

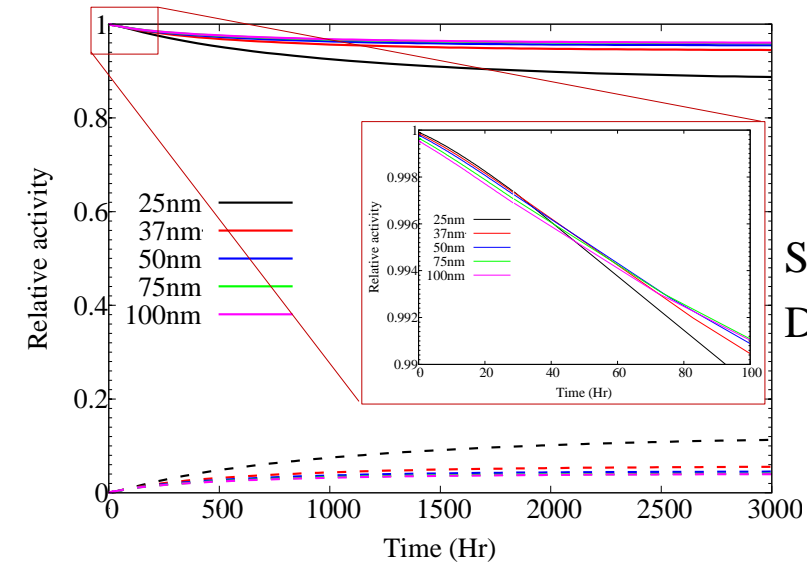
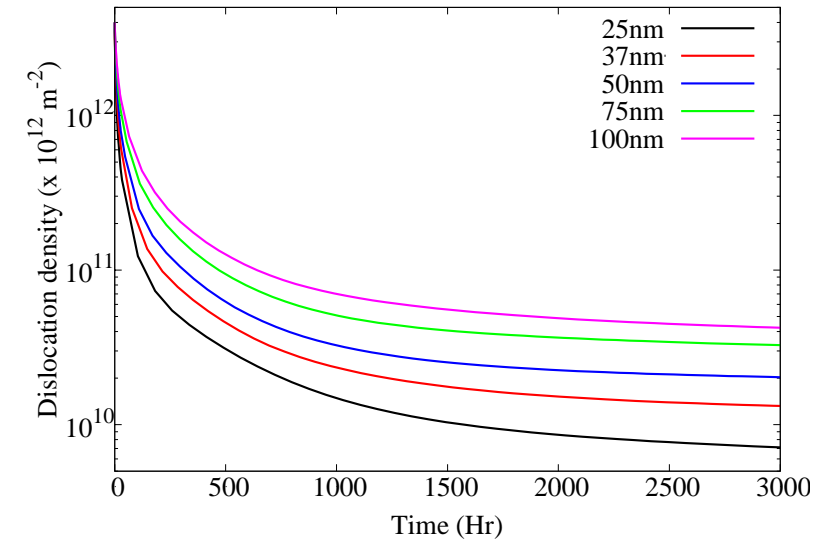


Precipitate “strengthening”

Gr91 subjected to creep at 600C under 100MPa stress

Increasing the size of precipitates which reduces the solute content in the matrix can lead to an increase in the creep rate

Increasing the size of promotes dislocation recovery thus benefiting the activation of diffusive processes (e.g. Nabarro Herring)



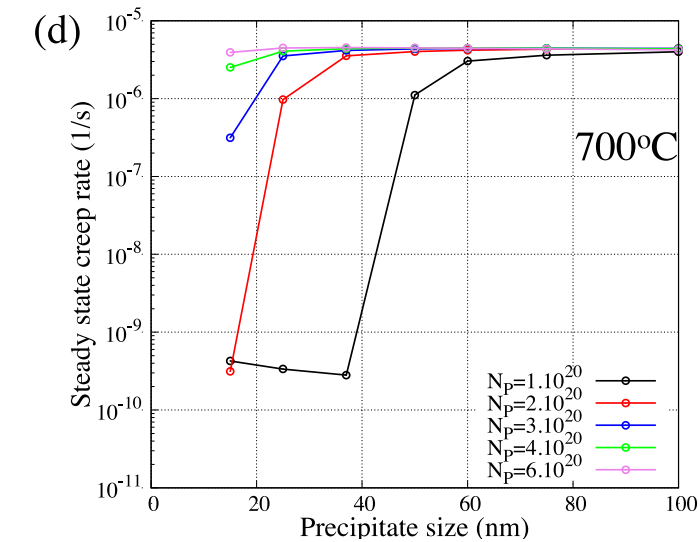
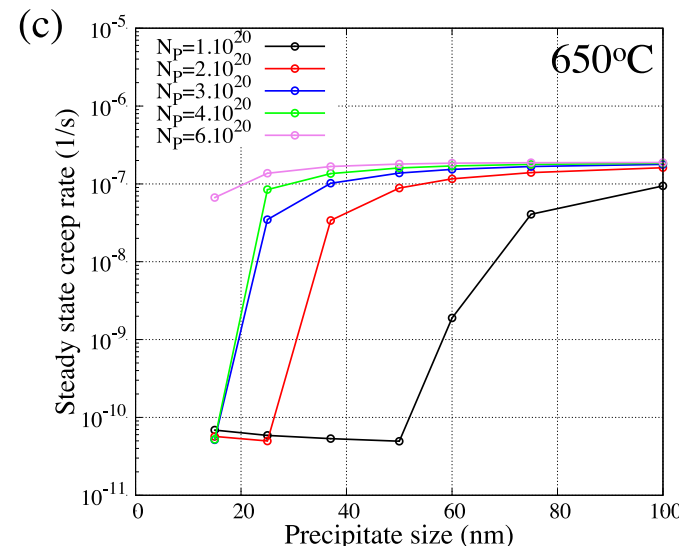
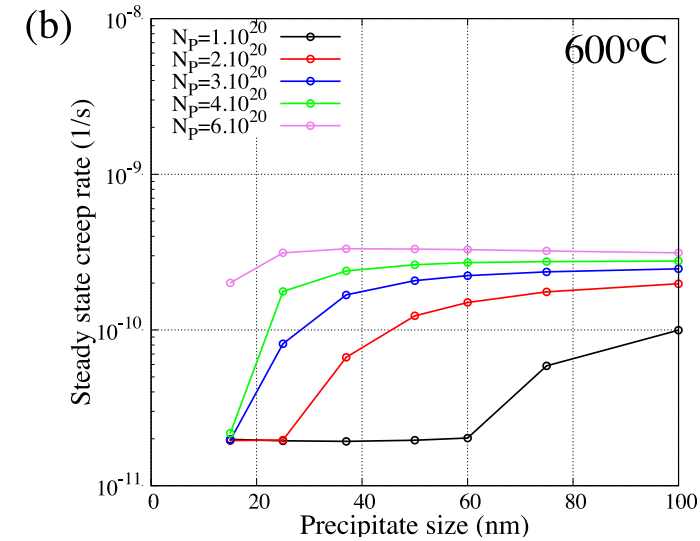
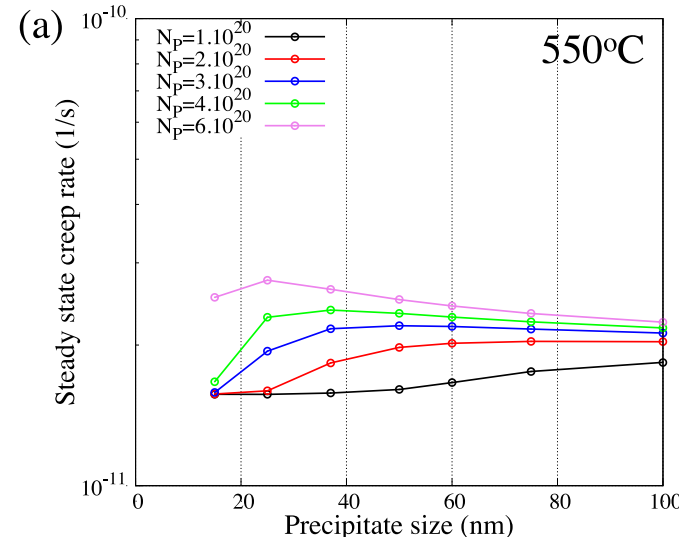
Solid: glide
Dashed: diffusion

Precipitate “strengthening”

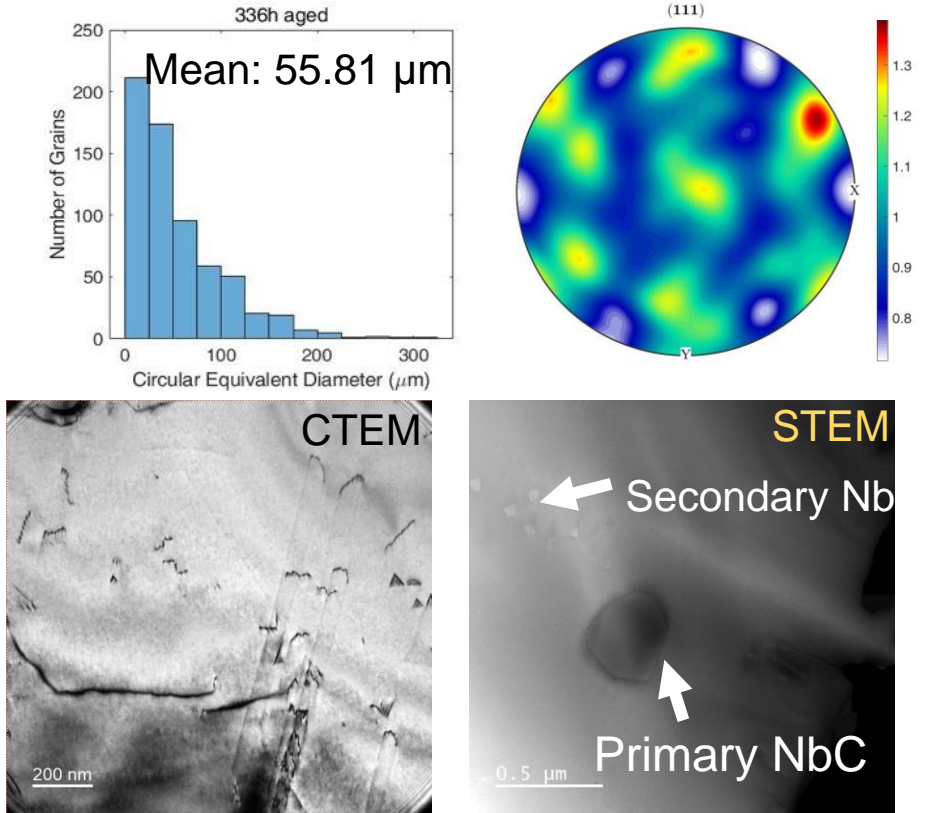
Increasing the size of precipitates which reduces the solute content in the matrix can lead to an increase in the creep rate.

Increasing the size of promotes dislocation recovery thus benefiting the activation of diffusive processes (e.g. Nabarro Herring).

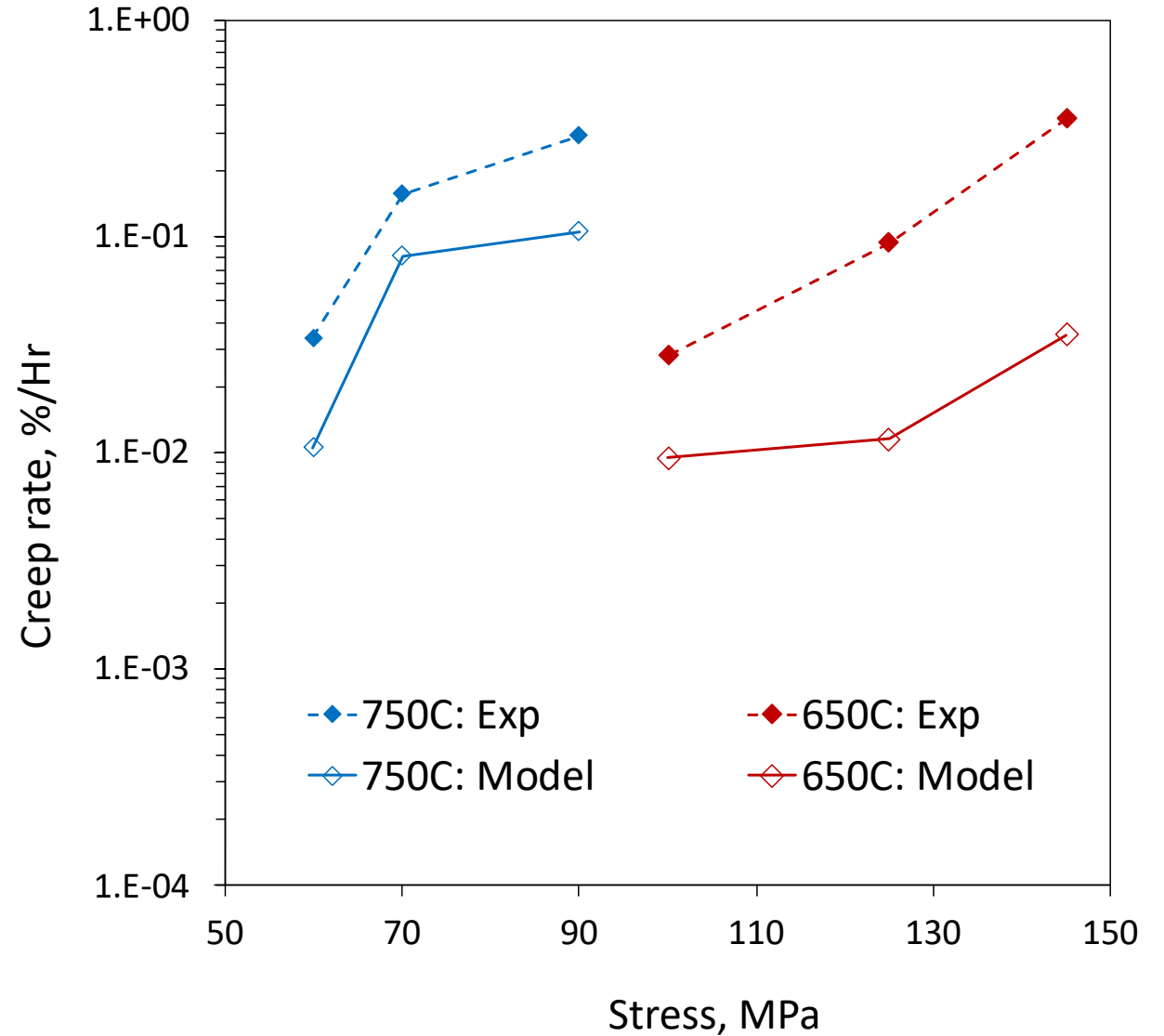
Overall the density and size of precipitates can either increase or decrease the steady state creep rate.



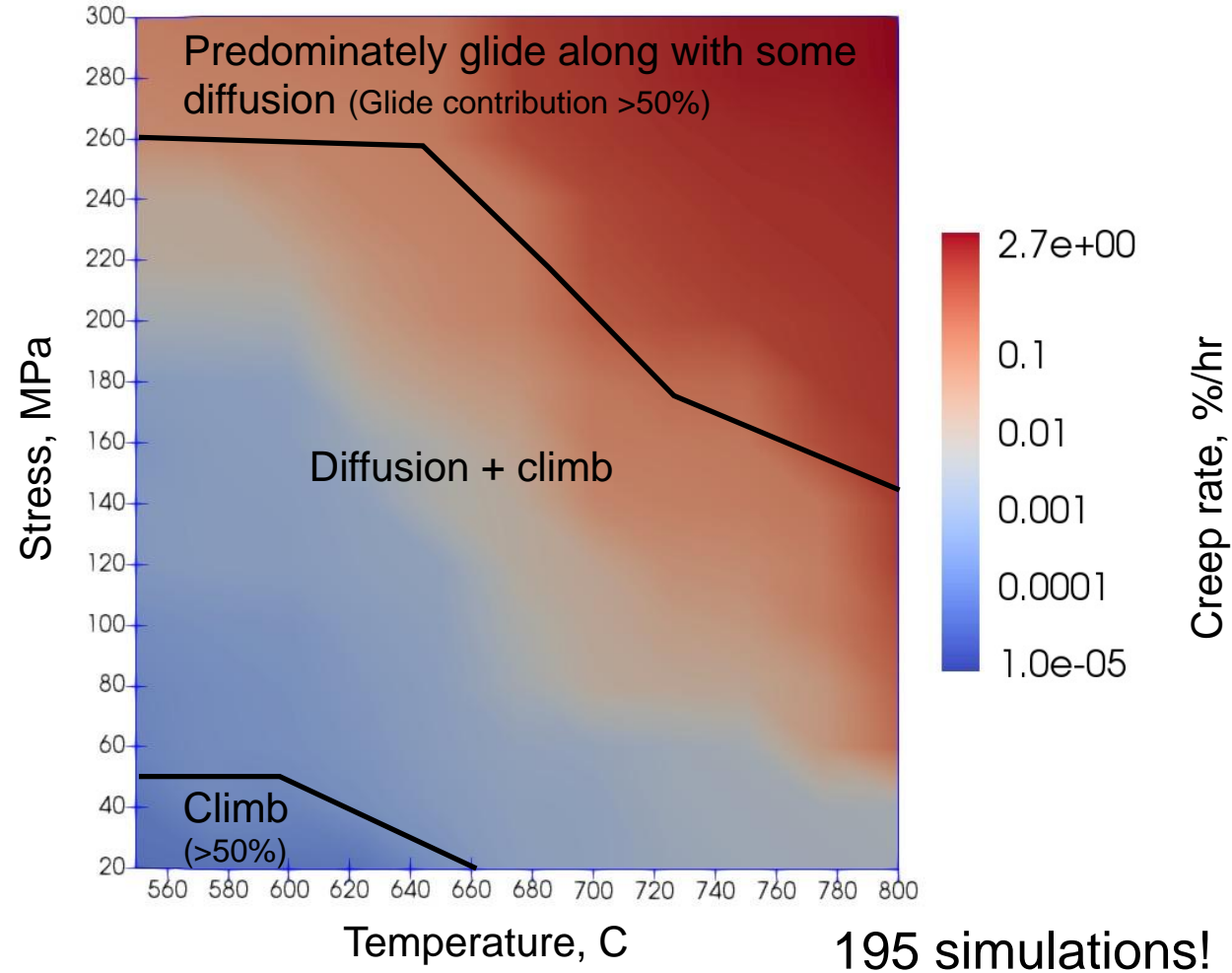
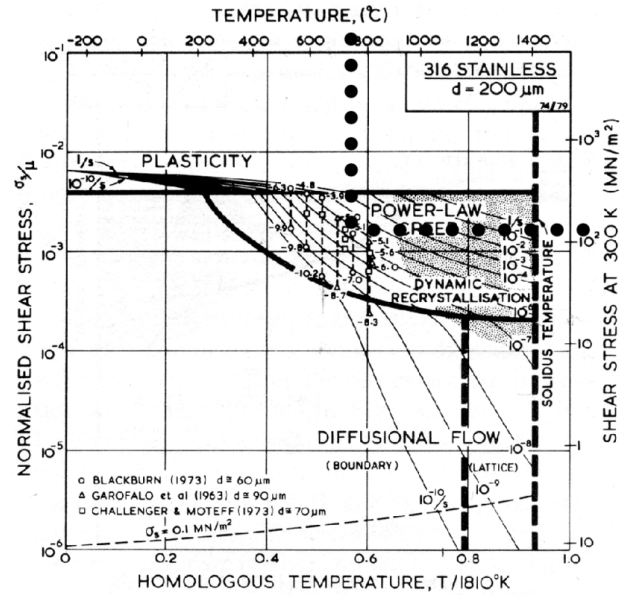
Effect of thermal aging on creep behavior: model vs experiments



Dislocation density: $\rho = 3.5 \pm 1.5 \times 10^{12} \text{m}^{-2}$
 Primary NbC: $N = 3.5 \times 10^{17} / \text{m}^3$, and $D = 330 \text{ nm}$
 Secondary NbC: $N = 2.5 \times 10^{19} / \text{m}^3$, and $D = 31.5 \text{ nm}$



LaMap: Synthetic deformation mechanisms map

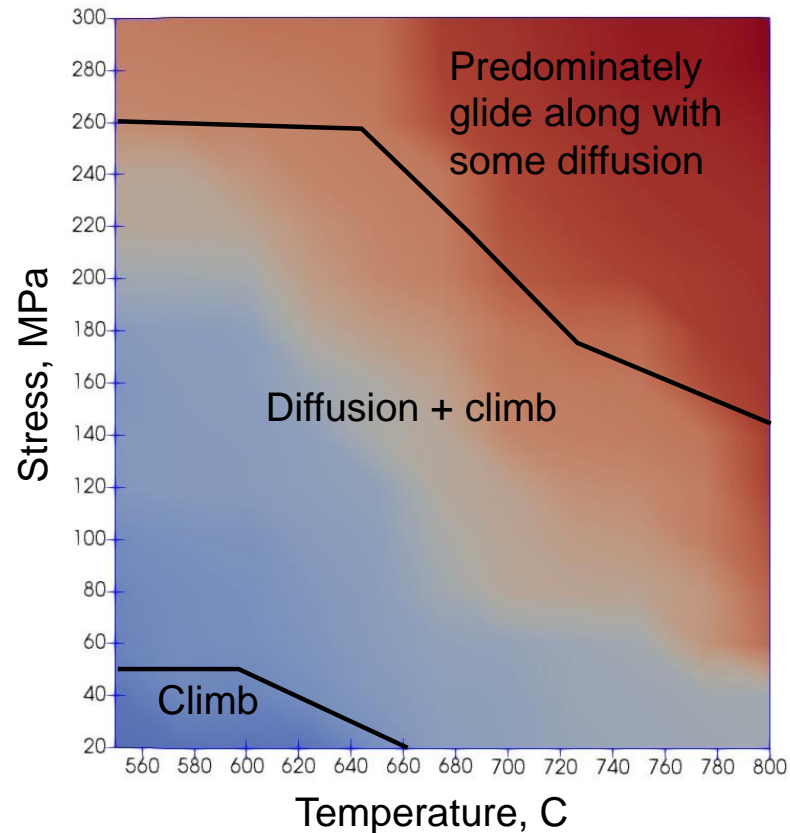


Effect of initial microstructure : Heat treatment

Base microstructure (case-1)

$$\rho_{ci} = 5 \times 10^{12} m^{-2}; \rho_{CW} = 1 \times 10^{11} m^{-2}$$

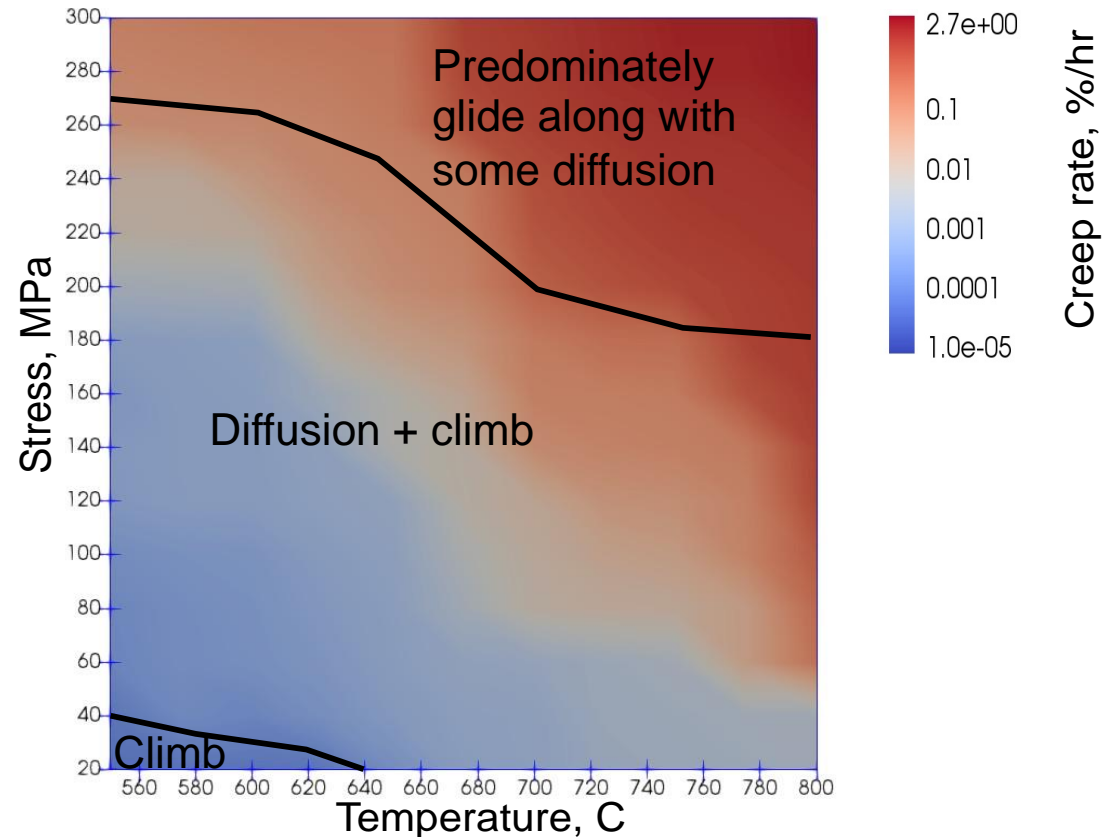
$$N_{NBC} = 3.5 \times 10^{17} m^{-3}; D_{NBC} = 330.0nm$$



Heat treated but not fully aged (case-2)

$$\rho_{ci} = 2 \times 10^{12} m^{-2}; \rho_{CW} = 1 \times 10^{11} m^{-2}$$

$$N_{NBC} = 3.5 \times 10^{17} m^{-3}; D_{NBC} = 330.0nm$$



Conclusion

Progress in developing a mechanistic polycrystal model.

Qualitative/ semi-quantitative effects of solute vs precipitate strengthening on creep response

